

# Spectral densities from Euclidean correlators via integral transforms: theoretical framework

---

L. Giusti<sup>a,b,c</sup>, M. Saccardi<sup>a,d</sup>, and D. Toniolo<sup>a,b</sup>

<sup>a</sup>*Dipartimento di Fisica, Università di Milano-Bicocca, Piazza della Scienza 3, I-20126 Milan, Italy*

<sup>b</sup>*INFN, Sezione di Milano-Bicocca, Piazza della Scienza 3, I-20126 Milan, Italy*

<sup>c</sup>*Theoretical Physics Department, CERN, 1211 Geneva 23, Switzerland*

<sup>d</sup>*Department of Physics, Colorado State University, Fort Collins, CO 80523, USA*

*E-mail:* [leonardo.giusti@unimib.it](mailto:leonardo.giusti@unimib.it), [matteo.saccardi@colostate.edu](mailto:matteo.saccardi@colostate.edu),  
[d.toniolo4@campus.unimib.it](mailto:d.toniolo4@campus.unimib.it)

ABSTRACT: Spectral densities link experimental measurements to dynamical properties of a quantum field theory which, in turn, can be resolved non-perturbatively from the Euclidean time-dependence of correlation functions. By making extensive use of integral transforms, we present analytic formulae to carry out the inverse Laplace transform so as to extract spectral densities from either the continuum or the discrete sampling of correlation functions in the Euclidean time. Formulae extend to regulated and/or smeared spectral densities as well. We explicitly show that the proposed lattice solution tends to its continuum counterpart up to  $O(a^2)$  effects in the lattice spacing  $a$  if the lattice correlator is  $O(a)$ -improved. In practical computations, lattices have necessarily a finite Euclidean temporal extent, a lack of knowledge which suggests to introduce incomplete integral transforms and the corresponding incomplete smeared spectral densities. The contribution from the unknowns to a smeared spectral density can then be rigorously bound and kept under control if the integral transform of the smearing function decays fast enough with the conjugate variable. Conversely, the bound can be used to plan lattices so as to achieve a given target precision on the reconstructed spectral density of interest. The formulae presented here in the context of lattice field theory can be easily applied or extended to other areas of research.

---

## Contents

<b>1</b>	<b>Introduction</b>	<b>1</b>
<b>2</b>	<b>Spectral densities from integral transforms</b>	<b>2</b>
2.1	Mellin transform	4
2.1.1	Spectral density	4
2.1.2	Regulated spectral density	4
2.2	Kontorovich–Lebedev and Mehler-Fock transforms	5
2.2.1	Spectral density	5
2.2.2	Regulated spectral density	6
<b>3</b>	<b>Smeared spectral densities</b>	<b>7</b>
3.1	Mellin case	8
3.2	Kontorovich–Lebedev case	8
<b>4</b>	<b>Smeared spectral densities from incomplete ones</b>	<b>9</b>
4.1	Incomplete Mehler-Fock transform	9
4.2	Incomplete spectral density	11
4.3	Incomplete smeared spectral densities	11
4.4	Smeared spectral densities	12
<b>5</b>	<b>Spectral densities from discrete sampling</b>	<b>14</b>
5.1	Spectral density	15
5.2	Regulated spectral density	16
5.3	Smeared spectral densities	17
<b>6</b>	<b>Smeared spectral densities from discrete incomplete ones</b>	<b>18</b>
6.1	Incomplete discrete Mehler-Fock transform	18
6.2	Incomplete spectral density from discrete sampling	19
6.3	Incomplete smeared spectral densities from discrete sampling	19
6.4	Smeared spectral densities from discrete sampling	20
<b>7</b>	<b>Discussion</b>	<b>22</b>
<b>8</b>	<b>Conclusions</b>	<b>25</b>
<b>A</b>	<b>Källén-Lehmann representation and spectral densities</b>	<b>26</b>
A.1	Spectral density as inverse Laplace transform	27
<b>B</b>	<b>Quasi-Carleman operators</b>	<b>27</b>
B.1	The Carleman operator	27
B.2	The quasi-Carleman operator for $r = 0$ and $\beta > 0$	29
B.3	The quasi-Carleman operator for $r > 0$ and $\beta = 0$	31

<b>C</b>	<b>Integral transforms</b>	<b>32</b>
C.1	Mellin transform	32
C.2	Kontorovich–Lebedev transform	33
C.3	Mehler-Fock transform	33
<b>D</b>	<b>Quasi-Carleman operators on discrete</b>	<b>34</b>
D.1	Hilbert matrix	34
D.2	Discretized quasi-Carleman operator for $r > 0$ and $\beta = 0$	35
D.3	Discretized quasi-Carleman operator for $r = 0$ and $\beta > 0$	36
<b>E</b>	<b>Alternative strategy for (smeared) regulated spectral densities</b>	<b>39</b>

---

## 1 Introduction

Spectral densities play a central rôle in field theories. They link dynamical properties of a theory to observables that can be measured in experiments. In the presence of strongly interacting fields, such as in Quantum Chromodynamics (QCD), non-perturbative computations of spectral densities from first principles are essential for a detailed comprehension of the dynamics of the theory, e.g. its particle and resonance content and their properties, and for the comparison against experimental results. Smeared spectral densities from physics-motivated kernels are interesting as well. These classes of observables give access to inclusive hadronic cross sections, semi-leptonic decay rates, or non-static properties of the quark-gluon plasma, to name a few (see for instance Refs. [1–6]).

Correlation functions of (composite) fields in Euclidean space-time are the primary quantities that are computed non-perturbatively on the lattice by Monte Carlo evaluations of path-integrals. Thanks to the Källén–Lehmann decomposition, two-point correlators are related to the corresponding spectral densities by a Laplace transform. The direct extraction of (smeared) spectral densities from lattice data thus entails the Inverse Laplace Transform (ILT) of correlators, a notorious difficult inverse problem. The conceptual, algorithmic and technological progress in lattice QCD, however, unlocked unprecedented levels of precision in modern numerical calculations [7, 8]. Correlation functions at larger and larger time-distances are becoming accessible thanks to more efficient statistical estimators and to the development of multi-level integration techniques in the presence of fermions [9–11]. Larger and larger lattices with a denser and denser spectrum of states are being simulated in master-field simulations [12–14]. Therefore, it has become interesting and timely to reconsider the direct extraction of (smeared) spectral densities from lattice data [3, 15, 16].

Recently, we have proposed explicit analytic formulae to extract smeared spectral densities from the Euclidean time-dependence of correlation functions [17]. By making extensive use of integral transforms, the aim of this paper is to generalize and extend these results so as to be able to extract regulated and/or smeared spectral densities from either the continuous or discrete sampling of correlation functions in the Euclidean time. We pay particular

attention to discretization effects and to rigorously bind the systematic uncertainties due to the finite extension of the time direction. The practical implementation of the strategy proposed here, and its first application to real lattice QCD data generated by a multi-level Monte Carlo will be presented in full details in a companion paper [18].

## 2 Spectral densities from integral transforms

In this paper we focus on two-point connected correlation functions in Euclidean space-time<sup>1</sup>

$$C(t) = \int \langle \mathcal{O}_1(t, \mathbf{x}) \mathcal{O}_2(0, \mathbf{0}) \rangle_c d^3 \mathbf{x}, \quad (2.1)$$

where  $\mathcal{O}_1$  and  $\mathcal{O}_2$  are two renormalized scalar fields<sup>2</sup>. Thanks to the Källén–Lehmann spectral decomposition, see Appendix A for the notation, two-point correlators are related to the corresponding spectral densities  $\rho(\omega)$  by the Laplace transform

$$C(t) = \int_0^\infty \rho(\omega) e^{-\omega t} d\omega. \quad (2.2)$$

The spectral density is a function of the energy  $\omega$ , with support over  $[\omega_0 > 0, \infty)$  in channels with a mass gap  $\omega_0$ , which encodes the dynamical information of the theory in the channel identified by the quantum numbers of the fields in Eq. (2.1). When combined with the short-distance (operator product expansion) analysis, these properties fix the asymptotic behaviour of correlation functions at the origin and at infinity to be

$$\lim_{t \rightarrow 0^+} C(t) = O(t^{-p}), \quad \lim_{t \rightarrow +\infty} C(t) = O(e^{-\omega_0 t}), \quad (2.3)$$

where  $p$  is close to an integer in QCD. This, together with Eq. (2.2), in turn implies that

$$\rho(\omega) \Big|_{\omega \in [0, \omega_0)} = 0, \quad \lim_{\omega \rightarrow +\infty} \rho(\omega) = O(\omega^{p-1}). \quad (2.4)$$

To determine the spectral density from the correlator, the Eq. (2.2) has to be inverted, or equivalently the ILT of the correlator has to be computed. For the clarity of the presentation, in the first part of this section we present a rather general scheme of how integral transforms can lead to the extraction of the spectral density. The underlying assumptions and the details of the particular transforms (e.g. basis functions, domain of integration, etc.) are fully spelled out in the following subsections.

---

<sup>1</sup>In the main sections of this paper we assume the time-momentum representation of correlators, omitting the momentum dependence from the notation, and consider the zero momentum case. Our results, however, are fully generic and applicable to non-zero momentum correlators defined in Appendix A. Note also that our derivation applies straightforwardly to higher  $n$ -point functions, involving multiple Euclidean-time separations [19, 20].

<sup>2</sup>Generalization to non-zero spin can be found in many textbooks, see for instance Ref. [2].

For the time being, given the asymptotic behaviours in Eqs. (2.3) and (2.4), let us assume that the correlator and the spectral density in Eq. (2.2) admit integral transforms, e.g. one of those in Appendix C, defined as

$$\bar{C}_s = \int C(t) \bar{u}_s(t) dt, \quad \hat{\rho}_s = \int \rho(\omega) \hat{u}_s(\omega) d\omega, \quad (2.5)$$

and their inverses, and that the basis functions  $\bar{u}_s(t)$  and  $\hat{u}_s(\omega)$  are related by

$$\lambda_s \hat{u}_s(\omega) = \int e^{-\omega t} \bar{u}_s(t) dt, \quad (2.6)$$

where  $\lambda_s$  is a numerical coefficient and  $s$  is the real conjugate variable, see below. By inserting Eq. (2.6) into the second of Eqs. (2.5), and then by using Eq. (2.2), it immediately follows that

$$\bar{C}_s = \lambda_s \hat{\rho}_s. \quad (2.7)$$

As a result, the basic integral equation (2.2) becomes an algebraic relation between the integral transforms of the correlator and of the spectral density provided  $\lambda_s \neq 0$  for all  $s$ . This is the main advantage for considering integral transforms in this context. If we require the orthogonality condition

$$\int \hat{u}_s^*(\omega) \hat{u}_{s'}(\omega) d\omega = \delta(s - s'), \quad (2.8)$$

then Eq. (2.6) leads to

$$\int \int \bar{u}_s^*(t) A(t + t') \bar{u}_{s'}(t') dt dt' = |\lambda_s|^2 \delta(s - s'), \quad (2.9)$$

where  $A(t + t')$  is the kernel of a (quasi) Carleman operator<sup>3</sup> defined in Eq. (B.2) of Appendix B. If the  $\bar{u}_s(t)$  are chosen to be eigenfunctions of  $A$ ,

$$\int A(t + t') \bar{u}_s(t') dt' = |\lambda_s|^2 \bar{u}_s(t), \quad (2.10)$$

then also the vectors  $\bar{u}_s(t)$  form an orthonormal basis and satisfy

$$\lambda_s^* \bar{u}_s(t) = \int e^{-t\omega} \hat{u}_s(\omega) d\omega. \quad (2.11)$$

Therefore, once the integral transform of the correlator is computed, by using the completeness relation

$$\int \hat{u}_s^*(\omega) \hat{u}_s(\omega') ds = \delta(\omega - \omega'), \quad (2.12)$$

the spectral density can be readily computed as

$$\rho(\omega) = \int \frac{\bar{C}_s}{\lambda_s} \hat{u}_s^*(\omega) ds. \quad (2.13)$$

Notice that typically  $|\lambda_s|$  decreases exponentially with  $s$  as well as  $|\bar{C}_s|$ , and a delicate cancellation between numerator and denominator is at work on the r.h.s. of Eq. (2.13).

---

<sup>3</sup>The (quasi) Carleman operators are real and they always admit a basis of real eigenvectors, see Appendix B for details. We prefer, however, to keep the discussion more general, and leave the possibility that the basis functions are complex.

## 2.1 Mellin transform

Maybe the simplest choice to implement the strategy outlined above is the Mellin transform, see Ref. [17] and references therein. In this subsection we first examine the case of correlators which are  $L^2(\mathbb{R}^+)$ . The corresponding spectral densities are  $L^2(\mathbb{R}^+)$  as well, and do not need to be regulated, see Appendix A. The more general case of regulated spectral densities follows.

### 2.1.1 Spectral density

If  $C(t) \in L^2(\mathbb{R}^+)$ , i.e.  $p < 1/2$  in Eq. (2.3), the basis functions and eigenvalues for the Mellin transform either for the correlator or for the spectral density are<sup>4</sup>

$$\bar{u}_s(t) = u_s(t) = \frac{t^{is}}{\sqrt{2\pi t}}, \quad \hat{u}_s(\omega) = u_s^*(\omega), \quad \lambda_s = \lambda_s = \Gamma\left(\frac{1}{2} + is\right), \quad s \in \mathbb{R}, \quad (2.14)$$

since the Carleman operator is the one given in Eq. (B.3), see Appendix B for more details. The Mellin transforms of the correlator and the spectral density read

$$\bar{C}_s = \int_0^\infty C(t) u_s(t) dt, \quad \hat{\rho}_s = \int_0^\infty \rho(\omega) u_s^*(\omega) d\omega, \quad (2.15)$$

and thanks to the analogous of Eq. (2.6), see Appendix B,

$$\lambda_s u_s^*(\omega) = \int_0^\infty e^{-\omega t} u_s(t) dt, \quad (2.16)$$

we have

$$\bar{C}_s = \lambda_s \hat{\rho}_s. \quad (2.17)$$

Notice that  $\bar{C}_s$  and  $\hat{\rho}_s$  are analytic in the strip of the complex plane where they exist, see for instance Refs. [21, 22]. The spectral density is then obtained as [17]

$$\rho(\omega) = \int_{-\infty}^{+\infty} \frac{\bar{C}_s}{\lambda_s} u_s(\omega) ds, \quad (2.18)$$

and, as anticipated, a delicate cancellation between numerator and denominator is at work.

### 2.1.2 Regulated spectral density

When in Eq. (2.3)  $p \geq 1/2$ , the Mellin transform of the correlator can be defined as

$$\bar{C}_{m,s} = \frac{1}{\sqrt{2\pi}} \int_0^\infty C(t) t^{m-1/2+is} dt = \int_0^\infty C(t) t^m u_s(t) dt, \quad m \in (p-1/2, +\infty), \quad (2.19)$$

where  $s \in \mathbb{R}$ , see Appendix C for more details. It amounts to multiplying  $C(t)$  by  $t^m$ , with  $m > p - 1/2$ , so that the resulting function is in  $L^2(\mathbb{R}^+)$  and can again be expanded on

---

<sup>4</sup>Notice the change in the sign of the label  $s$  when moving from the basis  $u_s(t)$  for the correlator to  $u_s^*(\omega) = u_{-s}(\omega)$  for the spectral density.

the basis of the  $u_s(t)$ . Analogously, the Mellin transform of the spectral density can be reformulated as

$$\hat{\rho}_{m,s} = \frac{1}{\sqrt{2\pi}} \int_0^\infty \rho(\omega) \omega^{-m-1/2-is} d\omega = \int_0^\infty \rho_m(\omega) u_s^*(\omega) d\omega, \quad m \in (p-1/2, +\infty), \quad (2.20)$$

and it corresponds to the Mellin transform of the regulated spectral density  $\rho_m(\omega) = \rho(\omega)/\omega^m \in L^2(\mathbb{R}^+)$ , see Appendix A, which again can be expanded on the basis of the  $u_s^*(\omega)$ . From Eq. (2.16) it follows

$$\lambda_{m,s} \omega^{-m} u_s^*(\omega) = \lambda_s \left(-\frac{\partial}{\partial \omega}\right)^m u_s^*(\omega) = \left(-\frac{\partial}{\partial \omega}\right)^m \int_0^\infty e^{-\omega t} u_s(t) dt = \int_0^\infty e^{-\omega t} t^m u_s(t) dt, \quad (2.21)$$

where  $\lambda_{m,s} = \Gamma(m + \frac{1}{2} + is)$ , which implies again that the basic integral equation (2.2) becomes an algebraic relation between the Mellin transforms of the correlator and of the spectral density

$$\bar{C}_{m,s} = \lambda_{m,s} \hat{\rho}_{m,s}. \quad (2.22)$$

By using the inversion formula in Eq. (C.3) of Appendix C, the regulated spectral density can finally be written as [17]

$$\rho_m(\omega) = \frac{\rho(\omega)}{\omega^m} = \int_{-\infty}^{+\infty} \frac{\bar{C}_{m,s}}{\lambda_{m,s}} u_s(\omega) ds, \quad m \geq 0. \quad (2.23)$$

## 2.2 Kontorovich–Lebedev and Mehler–Fock transforms

Lattice correlators are often affected by very large discretization effects at short time-distances. It is therefore appropriate to consider integral transforms defined by integrating over  $t \geq t_0 > 0$ . In this subsection we first examine the case of correlators with spectral densities which are  $L^1(\omega_0, \infty)$ , i.e.  $p < 0$  in Eq. (2.3), which do not need to be regulated to define the Kontorovich–Lebedev transform and its inverse. The more general case of regulated spectral densities follows.

### 2.2.1 Spectral density

When in Eq. (2.3)  $p < 0$ , the spectral density is  $L^1(\omega_0, \infty)$  and the Kontorovich–Lebedev transform and its inverse can be defined. The basis functions and eigenvalues for the related Mehler–Fock and Kontorovich–Lebedev transforms for the correlator and the spectral density are

$$\bar{u}_s(t) = \bar{u}_s(t, t_0) = \sqrt{\frac{s \tanh(\pi s)}{t_0}} {}_2F_1\left(\frac{1}{2} + is, \frac{1}{2} - is; 1; \frac{t_0 - t}{2t_0}\right), \quad \lambda_s = |\lambda_s|, \quad (2.24)$$

$$\hat{u}_s(\omega) = \hat{u}_s(\omega, t_0) = \frac{\sqrt{2s \sinh(\pi s)}}{\pi} \frac{K_{is}(\omega t_0)}{\sqrt{\omega}}, \quad t \geq t_0 > 0 \quad s \in \mathbb{R}^+, \quad (2.25)$$

where  ${}_2F_1$  and  $K_\nu$  are the Gauss’s hypergeometric function and the modified Bessel function of the second kind respectively [23], see Appendix B for more details. The corresponding quasi-Carleman operators are defined in Eqs. (B.31) and (B.17).

The Mehler-Fock and the Kontorovich–Lebedev transforms of the correlator and of the spectral density then read<sup>5</sup>

$$\bar{C}_s = \int_{t_0}^{\infty} C(t) \bar{u}_s(t, t_0) dt, \quad \hat{\rho}_s = \int_0^{\infty} \rho(\omega) \hat{u}_s(\omega, t_0) d\omega, \quad s \in \mathbb{R}^+, \quad (2.26)$$

while the analogous of Eq. (2.6), see Eq. (B.39) in Appendix B, becomes the “incomplete” Laplace transform

$$|\lambda_s| \hat{u}_s(\omega, t_0) = \int_{t_0}^{\infty} e^{-\omega t} \bar{u}_s(t, t_0) dt. \quad (2.27)$$

This implies that

$$\bar{C}_s = |\lambda_s| \hat{\rho}_s, \quad (2.28)$$

and the spectral density is then obtained as

$$\rho(\omega) = \int_0^{\infty} \frac{\bar{C}_s}{|\lambda_s|} \hat{u}_s(\omega, t_0) ds \quad (2.29)$$

where a delicate cancellation between numerator and denominator is again at work.

### 2.2.2 Regulated spectral density

When in Eq. (2.3)  $p \geq 0$ , we can apply the procedure of the previous subsection but on a suitably regulated correlator and spectral density. Following the standard line of argumentation summarized in Appendix A, we define the regulated correlator and spectral density as

$$C_m(t) = \int_0^{\infty} \rho_m(\omega) e^{-\omega t} d\omega, \quad \rho_m(\omega) = \frac{\rho(\omega)}{\omega^m}, \quad m > p. \quad (2.30)$$

By noticing that

$$\left(-\frac{\partial}{\partial t}\right)^m C_m(t) = C(t), \quad (2.31)$$

and that, in the presence of a mass gap, the regulated correlator and its derivatives are null at infinity, the  $C_m(t)$  can be written as

$$C_m(t) = \frac{1}{\Gamma(m)} \int_t^{\infty} C(t') (t' - t)^{m-1} dt', \quad m > 0, \quad (2.32)$$

while  $C_0(t) = C(t)$  for  $m = 0$ . The Mehler-Fock transform of  $C_m(t)$  reads

$$\bar{C}_{m,s} = \int_{t_0}^{\infty} C_m(t) \bar{u}_s(t, t_0) dt = \int_{t_0}^{\infty} C(t) \bar{u}_{m,s}(t, t_0) dt, \quad m \geq 0, \quad (2.33)$$

where  $\bar{u}_{0,s}(t, t_0) = \bar{u}_s(t, t_0)$  while, by using Eqs. (7.137.9) and (8.702) of Ref. [23],

$$\begin{aligned} \bar{u}_{m,s}(t, t_0) &= \frac{1}{\Gamma(m)} \int_{t_0}^t \bar{u}_s(t', t_0) (t - t')^{m-1} dt' \\ &= \sqrt{\frac{s \tanh(\pi s)}{t_0}} \frac{(t - t_0)^m}{\Gamma(m+1)} {}_2F_1\left(\frac{1}{2} + is, \frac{1}{2} - is; 1 + m; \frac{t_0 - t}{2t_0}\right), \quad m \geq 0. \end{aligned} \quad (2.34)$$

---

<sup>5</sup>We use the same notation for these transforms and the corresponding Mellin ones since any ambiguity is resolved from the context. The same applies to the regulated ones below. For the clarity of the notation, we leave the dependence on  $t_0$  implicit.

The Kontorovich–Lebedev transform of  $\rho_m(\omega)$  is

$$\hat{\rho}_{m,s} = \int_0^\infty \rho_m(\omega) \hat{u}_s(\omega, t_0) d\omega = \int_0^\infty \rho(\omega) \hat{u}_{m,s}(\omega, t_0) d\omega, \quad (2.35)$$

where

$$\hat{u}_{m,s}(\omega, t_0) = \frac{1}{\omega^m} \hat{u}_s(\omega, t_0), \quad (2.36)$$

and

$$|\lambda_s| \hat{u}_{m,s}(\omega, t_0) = \int_{t_0}^\infty e^{-\omega t} \bar{u}_{m,s}(t, t_0) dt, \quad (2.37)$$

with the last two equations which can also be explicitly derived by using Eqs. (8.702) and (7.141.5) of Ref. [23]. By inserting Eq. (2.30) into Eq. (2.33) and by using Eq. (2.37), it follows that

$$\bar{C}_{m,s} = |\lambda_s| \hat{\rho}_{m,s}, \quad (2.38)$$

and the regulated spectral density reads

$$\rho_m(\omega) = \int_0^\infty \frac{\bar{C}_{m,s}}{|\lambda_s|} \hat{u}_s(\omega, t_0) ds, \quad m \geq 0. \quad (2.39)$$

Notice that, if this very same procedure is adopted for the case of the Mellin transform, it leads to the results given in Section 2.1.2 where in particular  $\bar{u}_{m,s}$  is replaced by  $t^m u_s(t)$  up to a ratio of Gamma functions.

### 3 Smeared spectral densities

A smeared spectral density is defined by integrating a (regulated) density with a known kernel function  $\kappa(\omega)$ ,

$$\rho_{\kappa;m} = \int_0^\infty \rho_m(\omega) \kappa(\omega) d\omega. \quad (3.1)$$

Smeared spectral densities are interesting for several reasons. For physics-motivated kernels, they give access to phenomenologically relevant observables, such as inclusive hadronic cross sections or semi-leptonic decay rates to name a few (see for instance Refs. [3, 4, 24, 25]). From a more theoretical point of view, we have that often correlation functions are computed in a finite spatial volume. In those cases, the associated spectral densities are weighted sum of Dirac  $\delta$ -functions with possibly large spacings between successive levels. Integrating them with kernels which are representations of a Dirac  $\delta$ -function peaked around a certain energy  $\omega_*$  with a smearing width  $\sigma$  allows one to define the infinite volume limit smoothly [3]. For the clarity of the presentation, we first extend the general picture provided at the beginning of Section 2 by introducing a rather general scheme for computing smeared spectral densities via integral transforms. The discussion is later made precise for the Mellin and Kontorovich–Lebedev cases.

Let us assume that the smearing function  $\kappa(\omega)$  admits an integral transform defined as

$$\hat{\kappa}_s = \int \kappa(\omega) \hat{u}_s^*(\omega) d\omega. \quad (3.2)$$

By inserting the Eq. (2.13) into the Eq. (3.1) we arrive to the Parseval-like formula

$$\rho_\kappa = \int \hat{\rho}_s \hat{\kappa}_s ds = \int \frac{\overline{C}_s}{\lambda_s} \hat{\kappa}_s ds, \quad (3.3)$$

which can be directly used for the calculation of  $\rho_\kappa$ . The Eq. (3.3) may alternatively be derived by assuming that  $\kappa(\omega)$  admits not only the integral transform but also its inverse, i.e. satisfies the conditions described in Section 2. Then, by inserting the analogous of Eq. (2.13) for the smearing function into the Eq. (3.1), Eq. (3.3) is readily obtained. This way  $\rho_m(\omega)$  is only required to admit the integral transform, a condition that can be more easily met by spectral densities which become distributions at some finite value of  $\omega$ .

When a definite kernel is needed for illustration, in this paper we consider the Breit-Wigner smearing defined as

$$\kappa(\omega) = \frac{1}{\pi} \frac{\sigma}{(\omega - \omega_*)^2 + \sigma^2}, \quad (3.4)$$

while a more general discussion will be reported in Ref. [18].

### 3.1 Mellin case

Again the Mellin transform is maybe the simplest option for computing a smeared spectral density in the continuum. By following the line of argumentation presented above, we define

$$\hat{\kappa}_s = \int_0^\infty \kappa(\omega) u_s(\omega) d\omega. \quad (3.5)$$

By inserting the Eq. (2.23) into the Eq. (3.1) we then obtain

$$\rho_{\kappa;m} = \int_{-\infty}^{+\infty} \frac{\overline{C}_{m,s}}{\lambda_{m,s}} \hat{\kappa}_s ds, \quad m \geq 0, \quad (3.6)$$

where  $\overline{C}_{m,s}$  is defined in Eq. (2.19). For the Breit-Wigner, by using Eq. (3.197.1) of Ref. [23], the transform reads

$$\begin{aligned} \hat{\kappa}_s &= \frac{|\lambda_s|^2}{2\pi i} \left[ u_s(-\omega_* - i\sigma) - u_s(-\omega_* + i\sigma) \right] \\ &= \frac{1}{\cosh(\pi s)} \left[ \sqrt{\frac{b + \omega_*}{2b}} \cosh(s\vartheta) - i \sqrt{\frac{b - \omega_*}{2b}} \sinh(s\vartheta) \right] u_s(b), \end{aligned} \quad (3.7)$$

where  $b = \sqrt{\omega_*^2 + \sigma^2}$  and  $\cos \vartheta = -\frac{\omega_*}{b}$ .

### 3.2 Kontorovich–Lebedev case

For the case of the Kontorovich–Lebedev transform, we proceed analogously to the previous subsection. The transform of the smearing function is defined as

$$\hat{\kappa}_s = \int_0^\infty \kappa(\omega) \hat{u}_s(\omega, t_0) d\omega. \quad (3.8)$$

By inserting the Eq. (2.39) into the Eq. (3.1) we obtain

$$\rho_{\kappa;m} = \int_0^\infty \frac{\overline{C}_{m,s}}{|\lambda_s|} \hat{\kappa}_s ds, \quad m \geq 0, \quad (3.9)$$

where  $\overline{C}_{m,s}$  is defined in Eq. (2.33). For the Breit-Wigner, by using Eqs. (6.562.3) and (8.432.8) of Ref. [23], the Kontorovich–Lebedev transform reads

$$\begin{aligned} \hat{\kappa}_s = & \frac{\sqrt{s \sinh(\pi s) t_0}}{8\pi^2} \operatorname{Im} \left\{ 2 \left| \Gamma \left( -\frac{1}{4} + i \frac{s}{2} \right) \right|^2 {}_1F_2 \left( 1; \frac{5}{4} - i \frac{s}{2}, \frac{5}{4} + i \frac{s}{2}; \frac{(\omega_* + i\sigma)^2 t_0^2}{4} \right) + \right. \\ & + t_0 (\omega_* + i\sigma) \left| \Gamma \left( -\frac{3}{4} + i \frac{s}{2} \right) \right|^2 {}_1F_2 \left( 1; \frac{7}{4} - i \frac{s}{2}, \frac{7}{4} + i \frac{s}{2}; \frac{(\omega_* + i\sigma)^2 t_0^2}{4} \right) + \\ & \left. + 8\sqrt{2} \left| \Gamma \left( \frac{1}{2} + is \right) \right|^2 \frac{K_{is}(-(\omega_* + i\sigma)t_0)}{\sqrt{-(\omega_* + i\sigma)t_0}} \right\}, \end{aligned} \quad (3.10)$$

where  ${}_1F_2$  is a generalized hypergeometric series [23].

## 4 Smeared spectral densities from incomplete ones

Correlation functions are often known for  $0 \leq t \leq t_{\max}$  only<sup>6</sup>. It is therefore necessary to study the effect of this limitation on the extraction of (smeared) spectral densities. To this aim, from this section to the end of the paper, we focus on the Kontorovich–Lebedev and Mehler-Fock transforms since they are the continuum limit counterparts of those used in Section 5 for the ILT of correlation functions sampled on a discrete lattice. In particular, we introduce the incomplete Mehler-Fock transform and the incomplete (smeared) spectral densities, and scrutinize their behaviour. We then bind the difference between the target smeared spectral density and its incomplete counterpart so as to have a rigorous estimate of the systematic error associated to the ILT. An analogous (simpler) discussion can be applied to the Mellin transform as well.

### 4.1 Incomplete Mehler-Fock transform

When a correlation function is sampled on a finite temporal domain  $t_0 \leq t \leq t_{\max}$ , we have access to the incomplete Mehler-Fock transform

$$\tilde{C}_{m,s}(t_{\max}) = \int_{t_0}^{t_{\max}} C(t) \bar{u}_{m,s}(t, t_0) dt, \quad m \geq 0, \quad (4.1)$$

which differs from the complete one by

$$\overline{C}_{m,s} - \tilde{C}_{m,s}(t_{\max}) = \int_{t_{\max}}^\infty C(t) \bar{u}_{m,s}(t, t_0) dt. \quad (4.2)$$

---

<sup>6</sup>Throughout this paper we assume the interval  $0 \leq t \leq t_{\max}$  to be chosen so that the effects due to the boundary conditions in the time-direction are negligible. Otherwise, the additional systematics can be easily quantified by applying standard arguments.

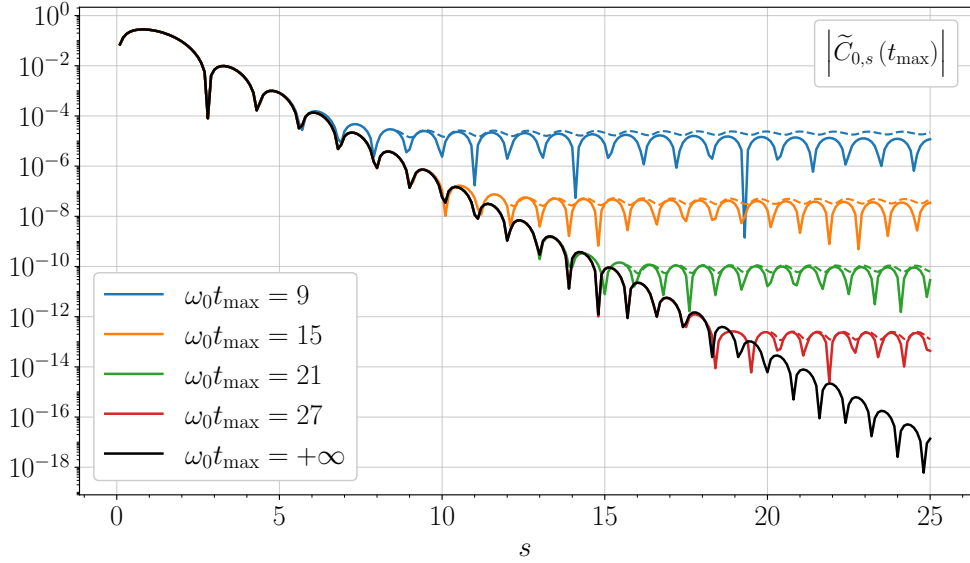


**Figure 1:** Absolute value of the complete (black) and incomplete Mehler-Fock transforms for  $m = 0$  of the function  $e^{-\omega_0 t}$  with  $\omega_0 = 0.9$  and  $t_0 = 1$  for various values of  $\omega_0 t_{\max}$ . The dashed lines represent the bounds obtained in Eq. (4.4) which, when  $|\bar{C}_{m,s}| \ll |\tilde{C}_{m,s}(t_{\max})|$ , de-facto binds  $|\tilde{C}_{m,s}(t_{\max})|$  too. The norm of the (incomplete) Mehler-Fock transform vanishes in the region of downward oscillations represented in the plot. However, for clarity, the  $s$ -grid has been chosen to avoid representing these zeros.

Thanks to Eq. (2.2) we can assume that, for large enough values of  $t_{\max}$ , it holds [17]

$$|C(t)| \leq |C(t_{\max})| e^{-\omega_0(t-t_{\max})}, \quad t \geq t_{\max}. \quad (4.3)$$

This implies that

$$\left| \bar{C}_{m,s} - \tilde{C}_{m,s}(t_{\max}) \right| \leq |C(t_{\max})| b_{m,s}(t_{\max}), \quad (4.4)$$

where<sup>7</sup>

$$b_{m,s}(t_{\max}) = \int_{t_{\max}}^{\infty} e^{-\omega_0(t-t_{\max})} |\bar{u}_{m,s}(t, t_0)| dt. \quad (4.5)$$

For asymptotically large values of  $t$ , it holds

$$\bar{u}_{m,s}(t, t_0) = 2 \frac{|\lambda_s|}{|\lambda_{m,s}|} t^m \left\{ \operatorname{Re} \left[ e^{i\phi_{m,s}} u_s(t) \right] + O\left(\frac{t_0}{t}\right) \right\}, \quad e^{i\phi_{m,s}} = \frac{\Gamma(is)}{|\Gamma(is)|} \frac{|\lambda_{m,s}|}{\lambda_{m,s}} \left(\frac{t_0}{2}\right)^{-is}, \quad (4.6)$$

leading to

$$b_{m,s}(t_{\max}) \leq \sqrt{\frac{2}{\pi}} \frac{|\lambda_s|}{|\lambda_{m,s}|} \frac{t_{\max}^m}{\omega_0 \sqrt{t_{\max}}} + \dots, \quad (4.7)$$

which in turn implies that the r.h.s of Eq. (4.4) is exponentially suppressed in  $t_{\max}$ . As a representative example, in Figure 1 we show the absolute value of the complete (black)

<sup>7</sup>The dependence of  $b_{m,s}(t_{\max})$  on  $\omega_0$  and  $t_0$  is omitted for the clarity of the notation.

and the incomplete Mehler-Fock transforms for  $m = 0$  of a single exponential  $C(t) = e^{-\omega_0 t}$  with  $\omega_0 = 0.9$  in units of  $t_0 = 1$  for various values of  $\omega_0 t_{\max}$  together with the bound in Eq. (4.4). Analogous results are obtained for higher values of  $m$  where, as expected from Eq. (4.7), a weak dependence on  $s$  is observed for  $b_{m,s}(t_{\max})$ . On the one hand the norm of the Mehler-Fock transform of a correlation function of the type considered in this paper, see Eq. (2.2), is expected to decrease exponentially with  $s$  up to harmful oscillations. On the other hand, the r.h.s of Eq. (4.4) is exponentially suppressed in  $t_{\max}$  but very weakly dependent on  $s$ . Therefore,  $\tilde{C}_{m,s}$  is an excellent approximation of  $\bar{C}_{m,s}$  when  $t_{\max}$  is large and  $s$  is small, see below. But the larger  $s$  gets, the worse the approximation becomes, until the delicate cancellation between the numerator and the denominator in the r.h.s. of Eq. (2.39) is not at work anymore if  $\bar{C}_{m,s}$  is approximated by  $\tilde{C}_{m,s}$  in that formula.

## 4.2 Incomplete spectral density

The previous considerations suggest to define an incomplete spectral density as

$$\rho_m(\omega, s_{\max}) = \int_0^{s_{\max}} \frac{\bar{C}_{m,s}}{|\lambda_s|} \hat{u}_s(\omega, t_0) ds, \quad m \geq 0, \quad (4.8)$$

which, for  $\omega = \omega_*$ , can also be interpreted as a smeared spectral density with smearing function

$$\kappa(\omega) = \int_0^{s_{\max}} \hat{u}_s(\omega_*, t_0) \hat{u}_s(\omega, t_0) ds. \quad (4.9)$$

Thanks to the upper cut-off  $s_{\max}$ , the replacement of  $\bar{C}_{m,s}$  with  $\tilde{C}_{m,s}$  is well justified, and therefore we introduce

$$\tilde{\rho}_m(\omega, s_{\max}) = \int_0^{s_{\max}} \frac{\tilde{C}_{m,s}(t_{\max})}{|\lambda_s|} \hat{u}_s(\omega, t_0) ds, \quad m \geq 0. \quad (4.10)$$

Its difference from  $\rho_m(\omega, s_{\max})$  satisfies

$$|\rho_m(\omega, s_{\max}) - \tilde{\rho}_m(\omega, s_{\max})| \leq \Delta \tilde{\rho}_m(\omega, s_{\max}), \quad (4.11)$$

where

$$\Delta \tilde{\rho}_m(\omega, s_{\max}) = |C(t_{\max})| \int_0^{s_{\max}} \frac{b_{m,s}(t_{\max}) |\hat{u}_s(\omega, t_0)|}{|\lambda_s|} ds \quad (4.12)$$

with the integral on the r.h.s that can be computed numerically. At asymptotically large values of  $s_{\max}$ , that integral scales approximatively proportionally to  $e^{\pi s_{\max}/2}/s_{\max}^m$ . Therefore, to meet a given absolute precision on the incomplete spectral density,  $s_{\max}$  *has to scale approximately proportionally to  $\omega_0 t_{\max}$* .

## 4.3 Incomplete smeared spectral densities

Analogously to the previous subsection, we can define the incomplete smeared spectral densities as

$$\rho_{\kappa;m}(s_{\max}) = \int_0^{s_{\max}} \frac{\bar{C}_{m,s}}{|\lambda_s|} \hat{\kappa}_s ds, \quad m \geq 0. \quad (4.13)$$

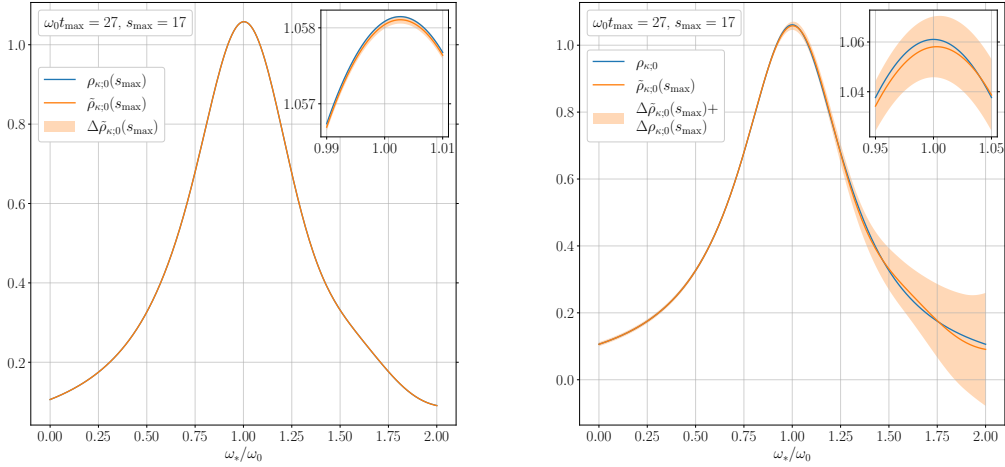


**Figure 2:** Left: The approximated incomplete smeared spectral density  $\tilde{\rho}_{\kappa;0}(s_{\max})$  with the error estimated as in Eq. (4.16), against the incomplete smeared spectral density  $\rho_{\kappa;0}(s_{\max})$  for the single exponential  $e^{-\omega_0 t}$  with  $\omega_0 = 0.9$ ,  $t_0 = 1$ . Right: The approximated incomplete smeared spectral density  $\tilde{\rho}_{\kappa;0}(s_{\max})$  with the total error estimated as in Eq. (4.26), against the exact smeared spectral density  $\rho_{\kappa;0}$  for the same exponential.

Also in this case, if we define

$$\tilde{\rho}_{\kappa;m}(s_{\max}) = \int_0^{s_{\max}} \frac{\tilde{C}_{m,s}(t_{\max})}{|\lambda_s|} \hat{\kappa}_s ds, \quad m \geq 0, \quad (4.14)$$

its difference from  $\rho_{\kappa;m}(s_{\max})$  satisfies

$$|\rho_{\kappa;m}(s_{\max}) - \tilde{\rho}_{\kappa;m}(s_{\max})| \leq \Delta\tilde{\rho}_{\kappa;m}(s_{\max}), \quad (4.15)$$

where

$$\Delta\tilde{\rho}_{\kappa;m}(s_{\max}) = |C(t_{\max})| \int_0^{s_{\max}} b_{m,s}(t_{\max}) \frac{|\hat{\kappa}_s|}{|\lambda_s|} ds, \quad (4.16)$$

and again the integral on the r.h.s can be computed numerically. As a representative example, in the left panel of Figure 2 we show  $\tilde{\rho}_{\kappa;0}(s_{\max})$  with its error, estimated as in Eq. (4.16), against  $\rho_{\kappa;0}(s_{\max})$  both extracted from the exponential considered in Section 4.1. The smearing function is a Breit-Wigner with  $\sigma = \omega_0/3$ .

#### 4.4 Smeared spectral densities

An incomplete smeared spectral density becomes a satisfactory approximation of the complete one if  $s_{\max} \sim \omega_0 t_{\max}$  is chosen large enough so as to guarantee a reconstruction error below the target precision. To quantify this systematics, we decompose a smeared density as

$$\rho_{\kappa;m} = \tilde{\rho}_{\kappa;m}(s_{\max}) + \left[ \rho_{\kappa;m}(s_{\max}) - \tilde{\rho}_{\kappa;m}(s_{\max}) \right] + \left[ \rho_{\kappa;m} - \rho_{\kappa;m}(s_{\max}) \right]. \quad (4.17)$$

The norm of the second term on the r.h.s of this equation is bounded by  $\Delta\tilde{\rho}_{\kappa;m}(s_{\max})$  in Eq. (4.16). We are therefore left to bind the difference between the target smeared spectral density and its incomplete counterpart. To do so, we notice that from Eqs. (2.38), (2.35) and (2.25) it follows

$$\begin{aligned} \left| \frac{\overline{C}_{m,s}}{\lambda_s} \right| &\leq \frac{\sqrt{2s \sinh(\pi s)}}{\pi} \int_0^\infty \left| \frac{\rho_m(\omega)}{\sqrt{\omega}} \right| |K_{is}(\omega t_0)| d\omega \\ &\leq \frac{\sqrt{2s \sinh(\pi s)}}{\pi} \max_{\omega \in \mathbb{R}^+} |K_{is}(\omega t_0)| r_m, \end{aligned} \quad (4.18)$$

where

$$r_m = \int_0^\infty \left| \frac{\rho_m(\omega)}{\sqrt{\omega}} \right| d\omega. \quad (4.19)$$

The modified Bessel function  $K_{is}(x)$  oscillates for  $x < s$  while it decays exponentially for  $x > s$  due to the change in nature of the differential equation it satisfies. As a consequence, its absolute maximum is the last peak of the oscillatory phase which occurs for  $x$  just below  $s$ . By assuming that  $\rho_m(\omega)$  and therefore  $C_m(t)$  have a definite sign, and by using Eq. (2.22) for  $s = 0$ ,  $r_m$  can be re-written as

$$r_m = \frac{1}{\Gamma(m + \frac{1}{2})} \int_0^\infty |C(t)| t^{m-1/2} dt. \quad (4.20)$$

The integral in Eq. (4.20) can be decomposed in the short-, intermediate- and long-distance contributions  $r_m^s$ ,  $r_m^i$  and  $r_m^l$  corresponding to integrating in the ranges  $[0, t_0]$ ,  $[t_0, t_{\max}]$ , and  $[t_{\max}, \infty]$  respectively. The short- and the intermediate-distance contributions can be bound or determined from the knowledge<sup>8</sup> of the correlator up to  $t_{\max}$ , respectively. By using Eq. (4.3), the long distance contribution satisfies

$$r_m^l \leq r_m^{l,\max} = \frac{e^{\omega_0 t_{\max}}}{\omega_0^{m+1/2}} \frac{\Gamma(m + \frac{1}{2}, \omega_0 t_{\max})}{\Gamma(m + \frac{1}{2})} |C(t_{\max})|, \quad (4.21)$$

with  $\Gamma(a, x)$  being the upper incomplete  $\Gamma$ -function which can easily be computed numerically [26]. For asymptotically large values of  $x$ , it holds

$$\Gamma(a, x) = x^{a-1} e^{-x} + \dots \quad (4.22)$$

leading to

$$r_m^{l,\max} = \frac{1}{\Gamma(m + \frac{1}{2})} \frac{t_{\max}^{m-1/2}}{\omega_0} |C(t_{\max})| + \dots \quad (4.23)$$

which is exponentially suppressed in  $t_{\max}$ . The difference between the smeared spectral density and the incomplete one can then be bounded as

$$\left| \rho_{\kappa;m} - \rho_{\kappa;m}(s_{\max}) \right| \leq \Delta\rho_{\kappa;m}(s_{\max}), \quad (4.24)$$

---

<sup>8</sup>For small enough values of  $t_0$ , perturbation theory is an interesting viable option to bind  $C(t)$  in  $[0, t_0]$ , and therefore  $r_m^s$ .

with

$$\Delta\rho_{\kappa;m}(s_{\max}) = r_m^{\max} \int_{s_{\max}}^{\infty} \frac{\sqrt{2s \sinh(\pi s)}}{\pi} \max_{\omega \in \mathbb{R}^+} |K_{is}(\omega t_0)| |\hat{\kappa}_s| ds, \quad (4.25)$$

where  $r_m^{\max}$  is the sum of the bounds on  $r_m^s$ ,  $r_m^i$  and  $r_m^l$ . By using Eqs. (4.16) and (4.25), it follows that

$$\left| \rho_{\kappa;m} - \tilde{\rho}_{\kappa;m}(s_{\max}) \right| \leq \Delta\tilde{\rho}_{\kappa;m}(s_{\max}) + \Delta\rho_{\kappa;m}(s_{\max}). \quad (4.26)$$

Therefore, the approximated incomplete smeared spectral density  $\tilde{\rho}_{\kappa;m}(s_{\max})$ , when supplemented by the systematic error  $[\Delta\tilde{\rho}_{\kappa;m}(s_{\max}) + \Delta\rho_{\kappa;m}(s_{\max})]$ , becomes a rigorous estimate of the smeared spectral density. As a representative example, in the right panel of Figure 2 we show  $\tilde{\rho}_{\kappa;0}(s_{\max})$  together with the total error, estimated as in Eq. (4.26), against  $\rho_{\kappa;0}$  both extracted from the exponential considered in subsection 4.1. The smearing function is the same Breit-Wigner used in the left panel of the same figure. If instead a Breit-Wigner with a varying width but with  $\sigma/\omega_*$  kept constant as a function of  $\omega_*$  was chosen, see Section 7, the error bound would have been more uniform as a function of  $\omega_*$ .

The  $s$ -dependence of the integrand in Eq. (4.25) is de-facto the one of the function  $|\hat{\kappa}_s|$ , since the remaining factor depends very weakly on  $s$ . Therefore, the dependence on  $s$  of the norm of the Kontorovich-Lebedev transform of the smearing function determines the rate of convergence to zero of  $\Delta\rho_{\kappa;m}(s_{\max})$  as a function of  $s_{\max}$ . As discussed in Section 4.1, when a correlation function is only known on a finite temporal domain  $t \leq t_{\max}$ , we have access to  $\bar{C}_{m,s}$  for  $s \leq s_{\max} \sim \omega_0 t_{\max}$  only, a lack of knowledge which prevents us to reconstruct exactly the (regulated) spectral density. If, however, we restrict ourselves to smeared spectral densities with  $|\hat{\kappa}_s|$  decaying fast enough with  $s$ , the effect of the unknowns can be bounded and kept under control. It is therefore wise to choose smearing functions with a fast decaying integral transform if the problem under investigation allows to do so. In this respect, the Breit-Wigner is a very conservative example since its transform decays approximatively as<sup>9</sup>  $1/s^2$ , but it has the advantage of having a simple expression which can be managed easily in the numerical examples considered in this paper.

## 5 Spectral densities from discrete sampling

When QCD is regularized on a lattice, the correlators are defined at discrete Euclidean times only,

$$\mathcal{C}(t_0 + an) = \int_0^{\infty} \varrho(\omega) e^{-\omega(t_0+an)} d\omega, \quad n = 0, 1, 2, \dots, \infty, \quad (5.1)$$

where  $a$  is the lattice spacing. Similarly to the continuum, the Eq. (5.1) must be inverted to extract the spectral density. We proceed by mimicking the derivation in Section 2.2 with  $t_0$  as a freely selectable parameter to leave open the possibility of avoiding potentially large discretization effects at short time-distances.

<sup>9</sup>A similar bound can be derived for the Mellin transform. In that case, the transform of the smearing function decays exponentially with  $s$ , see Eq. (3.7), and the bound on the error is tighter. However, in order to extract the spectral density, the Mellin transform requires the knowledge of  $C(t)$  in the interval  $[0, t_0]$  and not only to bind its contribution to the associated systematic error.

## 5.1 Spectral density

When a correlator is sampled on regularly-spaced discrete points, the Eqs. (2.26) are replaced by

$$\bar{\mathcal{C}}_s = a \sum_{n=0}^{\infty} \mathcal{C}(t_0 + an) \bar{v}_s(n, t_0, a), \quad \hat{\varrho}_s = \int_0^{\infty} \varrho(\omega) \hat{v}_s(\omega, t_0, a) d\omega, \quad s \in \mathbb{R}^+, \quad (5.2)$$

where  $t_0 = an_0$ , and the basis functions are related by the discretized version of Eq. (2.27), namely

$$|\lambda_s| \hat{v}_s(\omega, t_0, a) = a \sum_{n=0}^{\infty} e^{-\omega(t_0 + an)} \bar{v}_s(n, t_0, a). \quad (5.3)$$

From this equation it immediately follows

$$\bar{\mathcal{C}}_s = |\lambda_s| \hat{\varrho}_s, \quad (5.4)$$

which is exact at finite lattice spacing. Similarly to the continuum, if we require the orthogonality condition

$$\int_0^{\infty} \hat{v}_s(\omega, t_0, a) \hat{v}_{s'}(\omega, t_0, a) d\omega = \delta(s - s') \quad (5.5)$$

to hold, then Eq. (5.3) implies

$$a^2 \sum_{n, n'=0}^{\infty} \bar{v}_s(n, t_0, a) \mathcal{A}(n + n') \bar{v}_{s'}(n', t_0, a) = |\lambda_s|^2 \delta(s - s'), \quad (5.6)$$

a straightforward discretization of Eq. (2.9) with  $\mathcal{A}(n + n')$  being the kernel of the discretized quasi-Carleman operator defined in Eq. (D.12) of Appendix D. We then choose the  $\bar{v}_s(n, t_0, a)$  to be the eigenvectors of  $\mathcal{A}$

$$a \sum_{n'=0}^{\infty} \mathcal{A}(n + n') \bar{v}_s(n', t_0, a) = |\lambda_s|^2 \bar{v}_s(n, t_0, a), \quad (5.7)$$

which form a complete and orthonormal basis for the discretized functions in  $\ell^2(\mathbb{Z}^+)$ , see Appendix D for their definition and properties. Notice that, as expected, the eigenvalues  $|\lambda_s|^2$  of  $\mathcal{A}$  are the same as those of the continuum operator [27]. The spectral density can then be extracted as

$$\varrho(\omega) = \int_0^{\infty} \frac{\bar{\mathcal{C}}_s}{|\lambda_s|} \hat{v}_s(\omega, t_0, a) ds. \quad (5.8)$$

*Continuum limit at fixed  $t_0$*

To study the approach to the continuum limit of  $\varrho(\omega)$  at fixed  $t_0$ , we start by analyzing the leading discretization effects in  $\bar{\mathcal{C}}_s$  defined in Eq. (5.2). By assuming that discretization effects in  $\mathcal{C}(t_0 + an)$  start at  $O(a^2)$ , by using Eq. (D.22) in Appendix D, and by noticing that the trapezoidal rule is adopted in the first of Eqs. (5.2) up to a factor 1/2 in the first contribution to the sum, we obtain

$$\bar{\mathcal{C}}_s = \bar{\mathcal{C}}_s + \frac{a}{2} \mathcal{C}(t_0) \bar{u}_s(t_0, t_0) + \frac{a}{4t_0} \int_{t_0}^{\infty} \mathcal{C}(t) \left[ 1 + 2t \frac{\partial}{\partial t} \right] \bar{u}_s(t, t_0) dt + O(a^2), \quad (5.9)$$

where  $\bar{\mathcal{C}}_s$  is defined in Eq. (2.26). By integrating by parts the last integral, it follows that

$$\bar{\mathcal{C}}_s = \left[1 - \frac{a}{4t_0}\right] \bar{\mathcal{C}}_s - \frac{a}{2t_0} \int_{t_0}^{\infty} t \left[\frac{\partial}{\partial t} C(t)\right] \bar{u}_s(t, t_0) dt + O(a^2), \quad (5.10)$$

and by using Eq. (2.2) and integrating again by parts we finally arrive at

$$\bar{\mathcal{C}}_s = |\lambda_s| \left\{ \left[1 + \frac{a}{4t_0}\right] \hat{\rho}_s + \frac{a}{2t_0} \int_0^{\infty} \left[\omega' \frac{\partial}{\partial \omega'} \rho(\omega')\right] \hat{u}_s(\omega', t_0) d\omega' + O(a^2) \right\}. \quad (5.11)$$

Notice that, since both  $\bar{\mathcal{C}}_s$  and  $\bar{\mathcal{C}}_s$  are suppressed exponentially in  $s$ , discretization effects are suppressed exponentially in  $s$  as well. By inserting Eqs. (5.11) and (D.39) into Eq. (5.8) we obtain

$$\begin{aligned} \varrho(\omega) = & \left[1 - \frac{a}{2t_0} \omega \frac{\partial}{\partial \omega}\right] \rho(\omega) + \\ & + \frac{a}{2t_0} \int_0^{\infty} \left\{ \int_0^{\infty} \left[\omega' \frac{\partial}{\partial \omega'} \rho(\omega')\right] \hat{u}_s(\omega', t_0) d\omega' \right\} \hat{u}_s(\omega, t_0) ds + O(a^2). \end{aligned} \quad (5.12)$$

By assuming that the Kontorovich–Lebedev transform and its inverse exist not only for  $\rho(\omega)$  but also for  $\omega \frac{\partial}{\partial \omega} \rho(\omega)$ , we finally arrive to

$$\varrho(\omega) = \rho(\omega) + O(a^2), \quad (5.13)$$

which explicitly shows that the inversion procedure does not introduce  $O(a)$ -effects. If  $\mathcal{C}(t_0 + an)$  had no discretization effects and if  $\rho(\omega)$  admitted the transform and its inverse on the basis of the  $\hat{v}_s(\omega, t_0, a)$ , then the extracted spectral density would not be affected by discretization effects.

## 5.2 Regulated spectral density

The Eqs. (2.32) and (2.33) can be discretized as

$$\mathcal{C}_m(t_0 + an) = \frac{a}{\Gamma(m)} \sum_{n'=n}^{\infty} w_{n'-n} \mathcal{C}(t_0 + an') (an' - an)^{m-1}, \quad m > 0, \quad (5.14)$$

where  $w_0 = \frac{1}{2}$  and  $w_i = 1$  for  $i > 0$  to implement the trapezoidal rule<sup>10</sup>, and

$$\bar{\mathcal{C}}_{m,s} = a \sum_{n=0}^{\infty} \mathcal{C}_m(t_0 + an) \bar{v}_s(n, t_0, a) = a \sum_{n=0}^{\infty} \mathcal{C}(t_0 + an) \bar{v}_{m,s}(n, t_0, a), \quad m \geq 0, \quad (5.15)$$

where  $\mathcal{C}_0(t_0 + an) = \mathcal{C}(t_0 + an)$ ,

$$\bar{v}_{m,s}(n, t_0, a) = \frac{a}{\Gamma(m)} \sum_{n'=0}^n w_{n-n'} (an - an')^{m-1} \bar{v}_s(n', t_0, a), \quad (5.16)$$

and  $\bar{v}_{0,s}(n, t_0, a) = \bar{v}_s(n, t_0, a)$ . By defining

$$|\lambda_s| \hat{v}_{m,s}(\omega, t_0, a) = a \sum_{n=0}^{\infty} e^{-\omega(t_0+an)} \bar{v}_{m,s}(n, t_0, a), \quad (5.17)$$

<sup>10</sup>By changing the weights  $w_i$ , different Newton-Cotes rules could be implemented as well.

after some algebra it is possible to show that

$$\hat{v}_{m,s}(\omega, t_0, a) = \frac{1}{\omega^m} \hat{v}_s(\omega, t_0, a), \quad \frac{1}{\omega^m} = \frac{a}{\Gamma(m)} \left( -\frac{\partial}{\partial \omega} \right)^{m-1} \left[ \frac{1}{1 - e^{-a\omega}} - \frac{1}{2} \right], \quad (5.18)$$

and therefore we define

$$\hat{\varrho}_{m,s} = \int_0^\infty \varrho(\omega) \hat{v}_{m,s}(\omega, t_0, a) d\omega = \int_0^\infty \frac{\varrho(\omega)}{\omega^m} \hat{v}_s(\omega, t_0, a) d\omega. \quad (5.19)$$

Notice that, as in the continuum, the dependence on  $m$  and  $s$  in  $\hat{v}_{m,s}$  is factorized. By inserting Eq (5.1) into Eq. (5.15), it immediately follows that

$$\bar{\mathcal{C}}_{m,s} = |\lambda_s| \hat{\varrho}_{m,s}, \quad (5.20)$$

and therefore

$$\varrho_m(\omega) = \frac{\varrho(\omega)}{\omega^m} = \int_0^\infty \frac{\bar{\mathcal{C}}_{m,s}}{|\lambda_s|} \hat{v}_s(\omega, t_0, a) ds. \quad (5.21)$$

Since  $\omega^m/\omega^m = 1 + O(a^2)$ , in the continuum we recover the expected subtraction power and, by following the same line of argumentation of the previous section, it follows that

$$\varrho_m(\omega) = \rho_m(\omega) + O(a^2). \quad (5.22)$$

An alternative procedure to extract regulated spectral densities is discussed in Appendix E, where the starting point is to consider the correlator  $C(t) t^m$  and extract the corresponding spectral density with the formula analogous to Eq. (5.8). The latter is then linked to the target regulated spectral density, see Eqs. (E.3) and (E.4). When applied to discrete sampling, discretization effects are different with respect to the procedure described in this section.

### 5.3 Smearing spectral densities

For smeared spectral densities, we proceed analogously to Section 3.2. We define the transform of the smearing function as

$$\hat{k}_s = \int_0^\infty \kappa(\omega) \hat{v}_s(\omega, t_0, a) d\omega. \quad (5.23)$$

By inserting Eq. (5.21) into the analogous of Eq. (3.1) for  $\varrho_m$  we obtain<sup>11</sup>

$$\varrho_{\kappa;m} = \int_0^\infty \frac{\bar{\mathcal{C}}_{m,s}}{|\lambda_s|} \hat{k}_s ds, \quad m \geq 0, \quad (5.24)$$

where  $\bar{\mathcal{C}}_{m,s}$  is defined in Eq. (5.15).

---

<sup>11</sup>For a single exponential, an explicit check of discretization effects induced by the ILT reveals that for  $m = 0$  there are none, while for  $m > 0$  they are very moderate as expected from the expression of  $\omega^m/\omega^m$ . The more involved procedure in Appendix E removes them by construction.

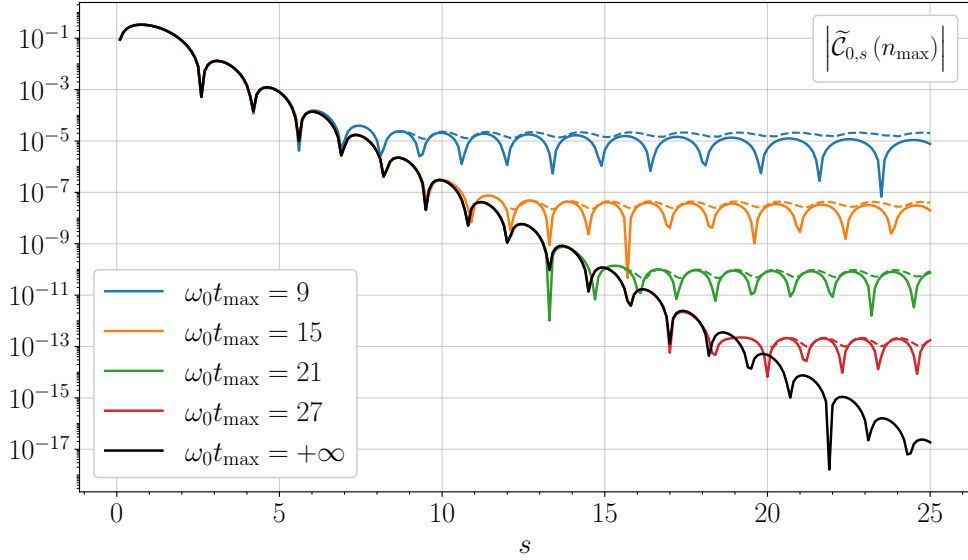


**Figure 3:** Absolute value of the complete (black) and incomplete discrete Mehler-Fock transforms for  $m = 0$  of the function  $e^{-\omega_0(t_0+an)}$  with  $a\omega_0 = 0.3$ ,  $t_0 = 3a$ , and  $t_{\max} = t_0 + an_{\max}$  for various values of  $\omega_0 t_{\max}$ . The dashed lines represent the bounds obtained from Eq. (6.4). As in the continuum, the norm of the (incomplete) discrete Mehler-Fock transform vanishes in the region of downward oscillations represented in the plot. However, for clarity, the  $s$ -grid has been chosen to avoid representing these zeros.

## 6 Smearing spectral densities from discrete incomplete ones

To compute a smeared spectral density from a discrete sampling of a correlator known for  $t_0 \leq t \leq t_{\max}$  only, we adapt the strategy outlined in Section 4 to the discrete case. In particular, we introduce the incomplete discrete Mehler-Fock transform and the corresponding incomplete (smeared) spectral density. We then bind the difference between the target smeared spectral density and its incomplete counterpart so as to have a rigorous estimate of the systematic uncertainty associated to the ILT.

### 6.1 Incomplete discrete Mehler-Fock transform

When a correlation function is sampled on regularly-spaced discrete points of a finite temporal domain  $t_0 \leq t \leq t_{\max}$ , we have access to the incomplete discrete Mehler-Fock transform

$$\tilde{\mathcal{C}}_{m,s}(n_{\max}) = a \sum_{n=0}^{n_{\max}} \mathcal{C}(t_0 + an) \bar{v}_{m,s}(n, t_0, a), \quad m \geq 0, \quad (6.1)$$

with  $an_{\max} = t_{\max} - t_0$ , which differs from the complete one by

$$\bar{\mathcal{C}}_{m,s} - \tilde{\mathcal{C}}_{m,s}(n_{\max}) = a \sum_{n=n_{\max}+1}^{\infty} \mathcal{C}(t_0 + an) \bar{v}_{m,s}(n, t_0, a). \quad (6.2)$$

Thanks to Eq. (5.1) we can assume that, for large enough values of  $n_{\max}$ , it holds

$$|\mathcal{C}(t_0 + an)| \leq |\mathcal{C}(t_0 + an_{\max})| e^{-a\omega_0(n-n_{\max})}, \quad n \geq n_{\max}. \quad (6.3)$$

This implies that

$$\left| \bar{\mathcal{C}}_{m,s} - \tilde{\mathcal{C}}_{m,s}(n_{\max}) \right| \leq \left| \mathcal{C}(t_0 + an_{\max}) \right| \mathbf{b}_{m,s}(n_{\max}), \quad (6.4)$$

where

$$\mathbf{b}_{m,s}(n_{\max}) = a \sum_{n=n_{\max}+1}^{\infty} e^{-a\omega_0(n-n_{\max})} |\bar{v}_{m,s}(n, t_0, a)|. \quad (6.5)$$

As a representative example, in Figure 3 we show the complete (black) and the incomplete discrete Mehler-Fock transforms for  $m = 0$  of a single exponential  $e^{-\omega_0(t_0+an)}$  with  $a\omega_0 = 0.3$  and  $t_0 = 3a$  for various values of  $\omega_0 t_{\max}$  together with the bound obtained from Eq. (6.4). Analogous results are obtained for higher values of  $m$ . Comments similar to those reported at the end of Section 4.1 apply also in this case. In particular the larger  $s$  gets, the worse  $\tilde{\mathcal{C}}_{m,s}$  approximates  $\bar{\mathcal{C}}_{m,s}$ , until the delicate cancellation between the numerator and the denominator in the r.h.s. of Eq. (5.21) is not at work anymore.

## 6.2 Incomplete spectral density from discrete sampling

The previous considerations suggest to define an incomplete spectral density as

$$\varrho_m(\omega, s_{\max}) = \int_0^{s_{\max}} \frac{\bar{\mathcal{C}}_{m,s}}{|\lambda_s|} \hat{v}_s(\omega, t_0, a) ds, \quad m \geq 0. \quad (6.6)$$

If we define

$$\tilde{\varrho}_m(\omega, s_{\max}) = \int_0^{s_{\max}} \frac{\tilde{\mathcal{C}}_{m,s}(n_{\max})}{|\lambda_s|} \hat{v}_s(\omega, t_0, a) ds, \quad m \geq 0, \quad (6.7)$$

its difference from  $\varrho_m(\omega, s_{\max})$  satisfies

$$\left| \varrho_m(\omega, s_{\max}) - \tilde{\varrho}_m(\omega, s_{\max}) \right| \leq \Delta \tilde{\varrho}_m(\omega, s_{\max}), \quad (6.8)$$

where

$$\Delta \tilde{\varrho}_m(\omega, s_{\max}) = \left| \mathcal{C}(t_0 + an_{\max}) \right| \int_0^{s_{\max}} \frac{\mathbf{b}_{m,s}(n_{\max}) |\hat{v}_s(\omega, t_0, a)|}{|\lambda_s|} ds \quad (6.9)$$

with the integral on the r.h.s that can be computed numerically.

## 6.3 Incomplete smeared spectral densities from discrete sampling

Analogously to the continuum, we can define the incomplete smeared spectral densities as

$$\varrho_{\kappa;m}(s_{\max}) = \int_0^{s_{\max}} \frac{\bar{\mathcal{C}}_{m,s}}{|\lambda_s|} \hat{k}_s ds, \quad m \geq 0, \quad (6.10)$$

where  $\hat{k}_s$  is defined in Eq. (5.23). Again, the truncation given by  $s_{\max}$  allows us to define

$$\tilde{\varrho}_{\kappa;m}(s_{\max}) = \int_0^{s_{\max}} \frac{\tilde{\mathcal{C}}_{m,s}(n_{\max})}{|\lambda_s|} \hat{k}_s ds, \quad m \geq 0. \quad (6.11)$$

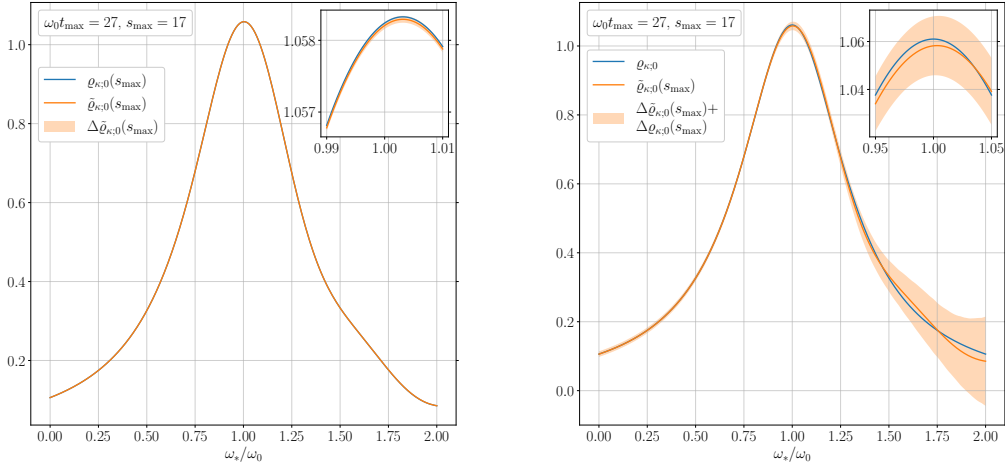


**Figure 4:** Left: The approximated incomplete smeared spectral density  $\tilde{\varrho}_{\kappa;0}(s_{\max})$  with the error estimated as in Eq. (6.13), against the incomplete smeared spectral density  $\varrho_{\kappa;0}(s_{\max})$  for the single exponential  $e^{-\omega_0(t_0+an)}$  with  $a\omega_0 = 0.3$  and  $t_0 = 3a$ . Right: The approximated incomplete smeared spectral density  $\tilde{\varrho}_{\kappa;0}(s_{\max})$  with the total error estimated as in Eq. (6.24), against the exact spectral density  $\varrho_{\kappa;0}$  for the same exponential.

Its difference from  $\varrho_{\kappa;m}(s_{\max})$  satisfies

$$\left| \varrho_{\kappa;m}(s_{\max}) - \tilde{\varrho}_{\kappa;m}(s_{\max}) \right| \leq \Delta \tilde{\varrho}_{\kappa;m}(s_{\max}), \quad (6.12)$$

where

$$\Delta \tilde{\varrho}_{\kappa;m}(s_{\max}) = \left| \mathcal{C}(t_0 + an_{\max}) \right| \int_0^{s_{\max}} \mathfrak{b}_{m,s}(n_{\max}) \frac{|\hat{k}_s|}{|\lambda_s|} ds, \quad (6.13)$$

and again the integral on the r.h.s can be computed numerically. As a representative example, in the left panel of Figure 4 we show  $\tilde{\varrho}_{\kappa;m}(s_{\max})$  with its error, estimated as in Eq. (6.13), against  $\varrho_{\kappa;m}(s_{\max})$  both extracted from the exponential considered in Section 6.1. The smearing function is a Breit-Wigner with  $\sigma = \omega_0/3$ .

#### 6.4 Smeared spectral densities from discrete sampling

Analogously to the continuum, an incomplete smeared spectral density becomes a satisfactory approximation of the complete one if  $\omega_0 t_{\max}$  is chosen large enough so as to guarantee a reconstruction error below the target precision. To quantify this systematics, we decompose a smeared density as<sup>12</sup>

$$\varrho_{\kappa;m} = \tilde{\varrho}_{\kappa;m}(s_{\max}) + \left[ \varrho_{\kappa;m}(s_{\max}) - \tilde{\varrho}_{\kappa;m}(s_{\max}) \right] + \left[ \varrho_{\kappa;m} - \varrho_{\kappa;m}(s_{\max}) \right]. \quad (6.14)$$

<sup>12</sup>A decomposition in which the three contributions are  $O(a)$ -improved independently is beyond the scope of this paper.

The norm of the second term on the r.h.s of this equation is bounded by  $\Delta\tilde{\varrho}_{\kappa;m}(s_{\max})$  in Eq. (6.13). To bind the difference between the target smeared spectral density and its incomplete counterpart, we notice that from Eqs. (D.25) and (D.31) it follows that

$$\begin{aligned} \left| \frac{\bar{\mathcal{C}}_{m,s}}{\lambda_s} \right| &\leq \frac{\sqrt{2s \sinh(\pi s)}}{\pi} \int_0^\infty |\varrho_m(\omega)| \frac{a}{\sqrt{1-e^{-a\omega}}} |\mathcal{K}_{is}(\omega, t_0)| d\omega \\ &\leq \frac{\sqrt{2s \sinh(\pi s)}}{\pi} \max_{\omega \in \mathbb{R}^+} |\mathcal{K}_{is}(\omega, t_0)| \mathfrak{r}_m, \end{aligned} \quad (6.15)$$

where

$$\mathcal{K}_{is}(\omega, t_0) = \sqrt{\frac{\pi}{a}} \left| \Gamma\left(2t_0/a - 1/2 + is\right) \right| \sqrt{\frac{e^{-a\omega}}{1-e^{-a\omega}}} P_{-\frac{1}{2}+is}^{1-2t_0/a} \left( \coth\left(\frac{a\omega}{2}\right) \right), \quad (6.16)$$

and

$$\mathfrak{r}_m = a \int_0^\infty |\varrho_m(\omega)| \sqrt{\frac{1}{1-e^{-a\omega}}} d\omega. \quad (6.17)$$

Analogously to the continuum the function  $\mathcal{K}_{is}(\omega, t_0)$  first oscillate and then it decays exponentially, and its absolute maximum can be easily computed numerically. By assuming that  $\varrho_m(\omega)$  and therefore  $\mathcal{C}(t_0 + an)$  has a definite sign, and by remembering that

$$\frac{1}{\sqrt{1-e^{-a\omega}}} = \sum_{n=0}^{\infty} (-1)^n \binom{-\frac{1}{2}}{n} e^{-a\omega n}, \quad (6.18)$$

we obtain

$$\mathfrak{r}_m = a \sum_{n=0}^{\infty} (-1)^n \binom{-\frac{1}{2}}{n} \mathcal{C}_m(an) = a \sum_{n=0}^{\infty} b_m^n \mathcal{C}(an), \quad (6.19)$$

where from Eq. (5.14)

$$b_m^n = \frac{a}{\Gamma(m)} \sum_{n'=0}^n w_{n-n'} (-1)^{n'} \binom{-\frac{1}{2}}{n'} (an - an')^{m-1}, \quad m \geq 1, \quad (6.20)$$

while for  $m = 0$  we use the expression in the middle of Eq. (6.19). Analogously to the continuum, the sum in Eq. (6.19) can be decomposed in the short-, intermediate- and long-distance contributions  $\mathfrak{r}_m^s$ ,  $\mathfrak{r}_m^i$  and  $\mathfrak{r}_m^l$  corresponding to sum in the ranges  $[0, t_0]$ ,  $[t_0, t_{\max}]$ , and  $[t_{\max}, \infty]$  respectively. For the short- and the intermediate-distance contributions considerations analogous to those in the continuum apply. By using Eq. (6.3), the long distance contribution satisfies

$$\mathfrak{r}_m^l \leq \mathfrak{r}_m^{l,\max} = |\mathcal{C}(an_{\max})| a \sum_{n=n_{\max}+1}^{\infty} b_m^n e^{-a\omega_0(n-n_{\max})}. \quad (6.21)$$

which is exponentially suppressed in  $n_{\max} = t_{\max}/a$ . The difference between the smeared spectral density and the incomplete one can then be bounded as<sup>13</sup>

$$\left| \varrho_{\kappa;m} - \varrho_{\kappa;m}(s_{\max}) \right| \leq \Delta\varrho_{\kappa;m}(s_{\max}), \quad (6.22)$$

<sup>13</sup>With a similar spirit, while we were completing this paper an approximation of these bounds was proposed in Ref. [28]. Additionally, explicitly enforcing the positivity of spectral functions recently allowed one to compute alternative bounds on their smeared counterpart [29–31].

with

$$\Delta \varrho_{\kappa;m}(s_{\max}) = \mathfrak{r}_m^{\max} \int_{s_{\max}}^{\infty} \frac{\sqrt{2s \sinh(\pi s)}}{\pi} \max_{\omega \in \mathbb{R}^+} \left| \mathcal{K}_{is}(\omega, t_0) \right| \left| \hat{k}_s \right| ds, \quad (6.23)$$

where  $\mathfrak{r}_m^{\max}$  is the sum of the bounds on  $\mathfrak{r}_m^s$ ,  $\mathfrak{r}_m^i$  and  $\mathfrak{r}_m^l$ . By using Eqs. (6.13) and (6.23) it follows that

$$\left| \varrho_{\kappa;m} - \tilde{\varrho}_{\kappa;m}(s_{\max}) \right| \leq \Delta \tilde{\varrho}_{\kappa;m}(s_{\max}) + \Delta \varrho_{\kappa;m}(s_{\max}). \quad (6.24)$$

Analogously to the continuum case, the approximated incomplete smeared spectral density  $\tilde{\varrho}_{\kappa;m}(s_{\max})$ , when supplemented by the systematic error  $[\Delta \tilde{\varrho}_{\kappa;m}(s_{\max}) + \Delta \varrho_{\kappa;m}(s_{\max})]$ , becomes a rigorous estimate of the smeared spectral density at finite lattice spacing. As a representative example, in the right panel of Figure 4 we show  $\tilde{\varrho}_{\kappa;m}(s_{\max})$  together with the total error, estimated as in Eq. (6.24), against  $\varrho_{\kappa;m}$  both extracted from the exponential considered in Subsection 6.1. Also in this case, the smearing function is a Breit-Wigner with  $\sigma = \omega_0/3$ .

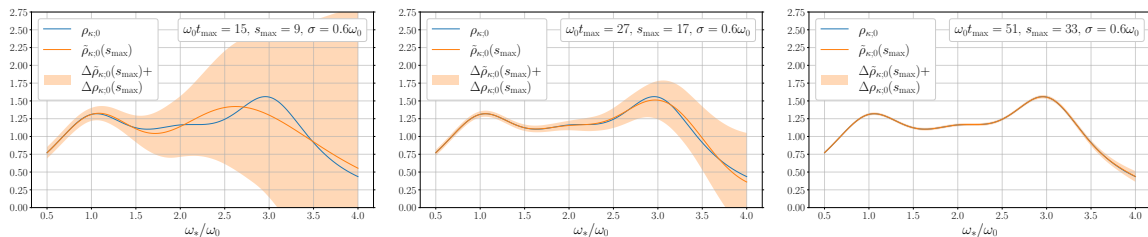
## 7 Discussion

When a correlator and the associated spectral density admit integral transforms and their inverses with basis functions related by an equation of the type (2.6), the basic integral equation in Eq. (2.2) becomes a simple algebraic relation among the integral transforms of the correlator and of the spectral density, see Eq. (2.7). The (smeared) spectral density is then readily obtained as an inverse transform. The key issue is the delicate cancellation between the numerator and the denominator in the integral on the r.h.s. of Eq. (2.13), i.e. between the exponential decay of the integral transform of the correlator as a function of the conjugate variable  $s$  and the exponentially decaying numerical coefficient in the denominator.

If the correlator is known for all  $t \geq t_0$ , the Laplace transform can be inverted exactly. In practical applications, however, the correlator is often known only up to  $t \leq t_{\max}$ . This implies that we only have access to an incomplete transform, see Eq. (4.1), due to the finiteness of the simulated lattice or possibly to the further limitation due to the worsening of the signal-to-noise ratio, see Ref. [18] for more details. At small values of  $s$ , the latter typically approximates the complete transform exponentially well in  $t_{\max}$ , see Figure 1. But when  $s \geq s_{\max} \sim \omega_0 t_{\max}$ , with  $\omega_0$  being the mass gap in that channel, the norm of the incomplete transform of the correlator does not decay exponentially with  $s$  anymore, a fact which prevents us from reconstructing exactly the (smeared) spectral density. This is clearly shown in Figure 1 for the Mehler-Fock transform, and an analogous plot can be obtained for the Mellin one.

This lack of knowledge implies that we have de-facto access to the incomplete smeared spectral density as defined in Eq. (4.13) only. If we restrict ourselves to smearing functions which have transforms decaying fast enough with  $s$ , however, the contributions of the unknowns to the smeared spectral density can be bounded and kept under control<sup>14</sup>, see

<sup>14</sup>An analogous line of argumentation can be applied to the study of finite volume effects. A complementary approach has been recently presented in Ref. [32].



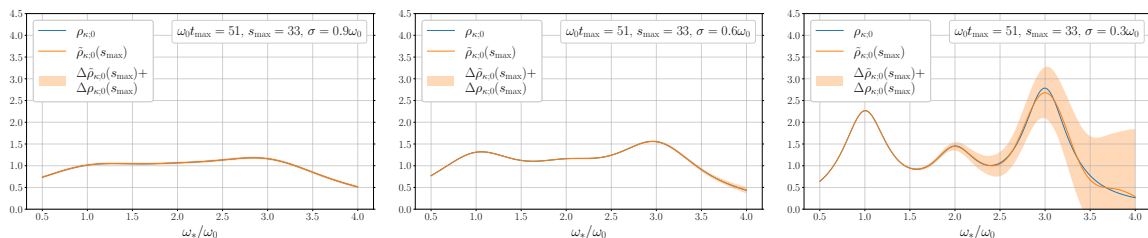
**Figure 5:** The approximated incomplete smeared spectral density  $\tilde{\rho}_{\kappa;0}(s_{\max})$  with the total error estimated as in Eq. (4.26), against the exact one  $\rho_{\kappa;0}$  for the correlator in Eq. (7.1) and for a Breit-Wigner smearing centered in  $\omega_*$  and with width  $\sigma/\omega_0 = 0.6$ . The three panels correspond to  $\omega_0 t_{\max} = 15$  (left), 27 (center) and 51 (right).

Figure 2. Very similar comments apply when the correlation function is sampled on discrete points only, as discussed in detail in Section 6.

It is instructive to scrutinize these findings for a simple example of a correlator made of a sum of 3 exponentials

$$C(t) = c_0 e^{-\omega_0 t} + c_1 e^{-\omega_1 t} + c_2 e^{-\omega_2 t} \quad (7.1)$$

with  $\omega_0 = 0.5$ ,  $\omega_1 = 1.0$ ,  $\omega_2 = 1.5$  and  $c_0 = 1.0$ ,  $c_1 = 0.5$ ,  $c_2 = 1.25$  in units of  $t_0 = 1$ . From this correlator we compute the spectral density smeared with the Breit-Wigner in Eq. (3.4) centered in  $\omega_*$  and with width  $\sigma$ . The Breit-Wigner is a very conservative example since its Kontorovich–Lebedev transform decays quite slowly as  $1/s^2$ , but it has the advantage that its transform has a simple expression which can be managed easily.



**Figure 6:** The approximated incomplete smeared spectral density  $\tilde{\rho}_{\kappa;0}(s_{\max})$  with the total error estimated as in Eq. (4.26), against the exact one  $\rho_{\kappa;0}$  for the correlator in Eq. (7.1) and for a Breit-Wigner smearing centered in  $\omega_*$  and with width  $\sigma/\omega_0 = 0.9$  (left), 0.6 (center), and 0.3 (right) for  $\omega_0 t_{\max} = 51$ .

In the three panels in Figure 5 we show the reconstructed smeared spectral density with constant width  $\sigma = 0.6\omega_0$  for three values of  $t_{\max}$  corresponding to  $\omega_0 t_{\max} = 15, 27$  and 51. By comparing the exact smeared spectral density (blue line) with the incomplete one (orange line), it is clear that the density can be reconstructed reliably with a rigorous bound of the systematic error attached to it. For the Breit-Wigner, the error decreases

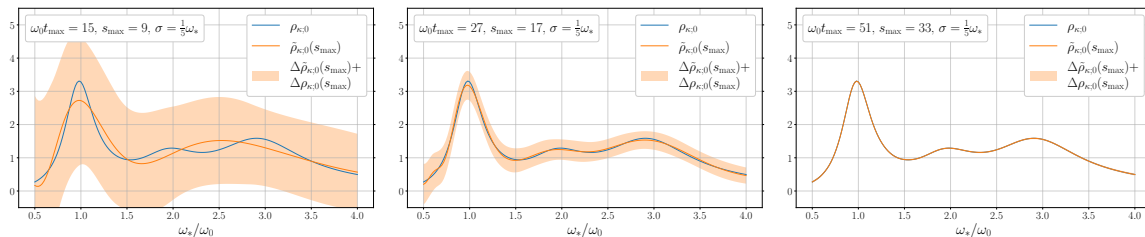


**Figure 7:** The approximated incomplete smeared spectral density  $\tilde{\rho}_{k;0}(s_{\max})$  with the total error estimated as in Eq. (4.26), against the exact one  $\rho_{k;0}$  for the correlator in Eq. (7.1) and for a Breit-Wigner smearing centered in  $\omega_*$  and with width  $\sigma/\omega_* = 1/5$ . The three panels correspond to  $\omega_0 t_{\max} = 15$  (left), 27 (center) and 51 (right).

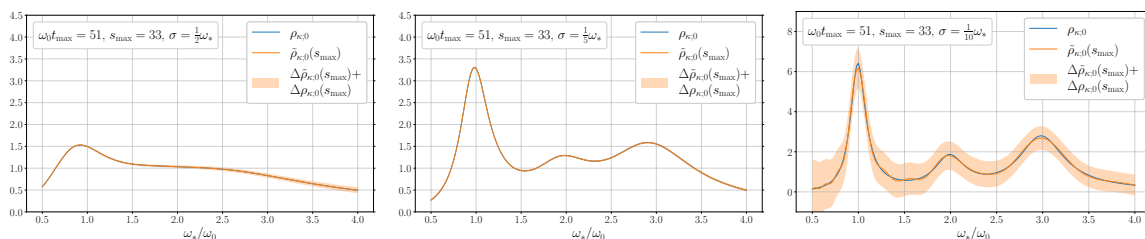


**Figure 8:** The approximated incomplete smeared spectral density  $\tilde{\rho}_{k;0}(s_{\max})$  with the total error estimated as in Eq. (4.26), against the exact one  $\rho_{k;0}$  for the correlator in Eq. (7.1) and for a Breit-Wigner smearing centered in  $\omega_*$  and with width  $\sigma/\omega_* = 1/2$  (left),  $1/5$  (center), and  $1/10$  (right, different scale on vertical axis) for  $\omega_0 t_{\max} = 51$ .

approximately as<sup>15</sup>  $s_{\max}^{-1} \sim (\omega_0 t_{\max})^{-1}$ , and it turns out to be quite loose. In the three panels in Figure 6 we show the very same reconstruction at fixed  $\omega_0 t_{\max} = 51$  but for three values of the smearing width  $\sigma/\omega_0 = 0.9, 0.6$  and  $0.3$ . As expected, the three-peak structure emerges when the smearing is smaller than the distance between the peaks, with the bound on the error that increases significantly.

In the three panels in Figure 7 we show, for  $\omega_0 t_{\max} = 15, 27$  and  $51$ , the reconstruction of the smeared spectral density with varying width but with the ratio  $\sigma/\omega_* = 1.5$  kept constant as a function of  $\omega_*$ . The error bound is more uniform as a function of  $\omega_*$  than in the panels of Figure 5. It is again clear that the spectral density can be reconstructed reliably with a rigorous estimate of the systematic error attached to it. Finally, in Figure 8 we show the very same reconstruction at fixed  $\omega_0 t_{\max} = 51$  but for three values of the ratio  $\sigma/\omega_* = 1/2, 1/5$  and  $1/10$ . As expected, the three-peak structure emerges when the smearing gets smaller and, at variance of the analogous plots in Figure 6, the error bound is more uniform as a function of  $\omega_*$ .

If one or a few leading exponential states are known, then they can be treated exactly

<sup>15</sup>The choice of the value of  $s_{\max}$  gives a handle to minimize the error in Eq. (4.26) by balancing the two competing contributions. In the simple examples shown in this section we have not extensively exploited this possibility.

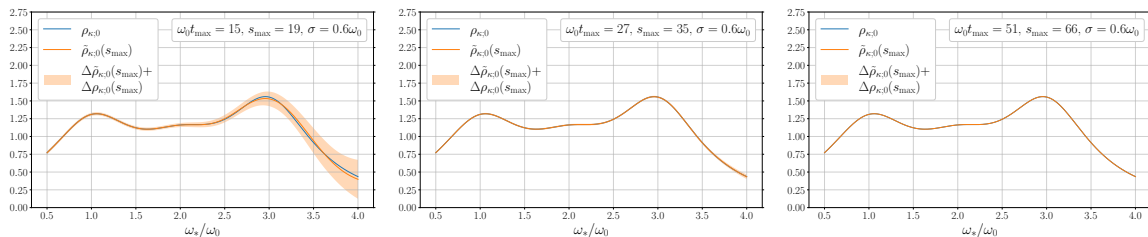


**Figure 9:** The approximated incomplete smeared spectral density  $\tilde{\rho}_{\kappa;0}(s_{\max})$  with the total error estimated as in Eq. (4.26) computed by preconditioning the correlator as explained in the main text, against the exact one  $\rho_{\kappa;0}$  for the correlator in Eq. (7.1) and for a Breit-Wigner smearing centered in  $\omega_*$  and with width  $\sigma/\omega_0 = 0.6$ . The three panels correspond to  $\omega_0 t_{\max} = 15$  (left), 27 (center) and 51 (right).

and all considerations above apply to the “preconditioned” correlation function, i.e. the correlation function subtracted by the known exponentials [33, 34]. In the three panels in Figure 9 we show the reconstructed smeared spectral density with constant width  $\sigma = 0.6\omega_0$  for three values of  $t_{\max}$  corresponding to  $\omega_0 t_{\max} = 15, 27$  and 51 obtained by subtracting the leading exponential, by computing the spectral density, and then by adding back the contribution of the leading exponential to the smeared spectral density. When compared with the three panels in Figure 5, the gain is substantial and approximatively as expected. This time the relevant parameter is  $s_{\max} \sim \omega_1 t_{\max}$  which is twice the one without preconditioning. When the correlator is computed numerically, however, whether this is an advantage depends on how much  $t_{\max}$  needs to be reduced once the leading exponential(s) has (have) been subtracted from the original correlator.

## 8 Conclusions

Integral transforms offer a powerful theoretical framework to compute the inverse Laplace transform of a correlator and to study the associated systematics. Leading discretization effects, systematics due to a finite temporal extent or to a finite spatial volume can be disentangled and studied independently on the lattice and in the continuum, respectively.

The solution proposed here, based on the Mehler-Fock and Kontorovich–Lebedev transforms, guarantees that a spectral density extracted from an  $O(a)$ -improved lattice correlator is  $O(a)$ -improved as well. In practical applications, the correlator is known on a finite time-interval only, e.g. up to  $t \leq t_{\max}$ . This implies that we can only have access to an incomplete transform of the correlator and therefore to an incomplete smeared spectral density. However, if the transform of the smearing function decays fast enough with the conjugate variable  $s$ , the unknown contributions can be bound and kept under control.

Here we have presented a generic derivation of the associated error bound. Depending on the particular physics application one is interested in, better bounds could be found by accelerating the convergence to zero of the transform of the smearing function, by deriving a more sophisticated formula for the bound, and/or by preconditioning the correlation function. Once all these optimizations are done, the improvement of the reconstruction requires

measuring the correlator at larger and larger time-distances. This can be achieved by enhancing the signal-to-noise ratio of the estimators of the correlators by variance reduction techniques such as the multi-level Monte Carlo integration.

## Acknowledgments

We thank M. Bruno for many discussions on the techniques and the phenomenological applications of spectral density reconstruction. This work is (partially) supported by ICSC - Centro Nazionale di Ricerca in High Performance Computing, Big Data and Quantum Computing, funded by European Union – NextGenerationEU. M.S. has been partially supported by the Italian *Fondazione Angelo Della Riccia*.

## A Källén-Lehmann representation and spectral densities

In this appendix we collect well-known formulas for subtracted dispersive relations in order to fix our notation and conventions for regulated spectral densities. We focus on two-point connected correlation functions in Euclidean space-time of the form

$$C(x) = \langle \mathcal{O}_1(x) \mathcal{O}_2(0) \rangle_c, \quad (\text{A.1})$$

where  $\mathcal{O}_1$  and  $\mathcal{O}_2$  indicate two renormalized scalar fields<sup>16</sup>. Thanks to the Källén-Lehmann spectral decomposition, we can define

$$\Pi(p^2) = \int C(x) e^{-ipx} d^4x = \int_0^\infty \frac{\rho(\sqrt{s})}{p^2 + s} ds, \quad p = (p_0, \mathbf{p}), \quad (\text{A.2})$$

where  $\rho(\sqrt{s})$  is the spectral density associated to the correlator  $C(x)$  which has support over  $[\sqrt{s} \geq \omega_0 > 0, \infty)$  if the sector has a mass gap  $\omega_0$ . Being an integrated correlation function,  $\Pi(p^2)$  can suffer from ultraviolet divergences. They can be removed by subtracting local counter terms to the correlation function, i.e. by defining the  $m$ -time subtracted function  $\Pi_m(p^2)$  ( $m = 1, 2, \dots$ ) as

$$\Pi(p^2) = \sum_{k=0}^{m-1} c_k (-p^2)^k + (-p^2)^m \Pi_m(p^2), \quad (\text{A.3})$$

where

$$\Pi_m(p^2) = \int_0^\infty \frac{\rho_{2m}(\sqrt{s})}{p^2 + s} ds, \quad \rho_m(\sqrt{s}) = \frac{\rho(\sqrt{s})}{(\sqrt{s})^m}, \quad c_k = \int_0^\infty \frac{\rho(\sqrt{s})}{s^{k+1}} ds, \quad (\text{A.4})$$

with  $\rho_m(\sqrt{s})$  being the regulated spectral density. Each coefficient  $c_k$  is, up to a sign, the derivative of order  $k$  of  $\Pi(p^2)$  with respect to  $p^2$  computed at  $p^2 = 0$ .

<sup>16</sup>Generalizations to non-zero spin fields can be found in many textbooks, see for instance Ref. [2].

## A.1 Spectral density as inverse Laplace transform

By introducing the time-momentum representation of the correlator

$$C(x_0, \mathbf{p}) = \int C(x) e^{-i\mathbf{p}\mathbf{x}} d^3\mathbf{x}, \quad x = (x_0, \mathbf{x}), \quad (\text{A.5})$$

by using Eq. (A.2) and the known integral [23]

$$\int_{-\infty}^{\infty} \frac{e^{ip_0x_0}}{p_0^2 + \omega^2} \frac{dp_0}{2\pi} = \frac{1}{2\omega} e^{-\omega|x_0|}, \quad (\text{A.6})$$

it is easy to show that

$$C(x_0, \mathbf{p}) = \int_{\sqrt{\mathbf{p}^2}}^{\infty} e^{-\omega x_0} \rho(\sqrt{\omega^2 - \mathbf{p}^2}) d\omega, \quad x_0 \geq 0, \quad (\text{A.7})$$

In Euclidean space-time, the spectral density can thus be extracted as the ILT of the time-momentum representation of the correlator. Following the same line of argumentation, one can relate the subtracted correlators in the time-momentum representation with the regulated spectral densities as

$$C_{2m}(x_0, \mathbf{p}) = \int_{-\infty}^{\infty} \frac{dp_0}{2\pi} e^{ip_0x_0} \int_0^{\infty} \frac{\rho_{2m}(\sqrt{s})}{p_0^2 + \mathbf{p}^2 + s} ds = \int_{\sqrt{\mathbf{p}^2}}^{\infty} e^{-\omega x_0} \rho_{2m}(\sqrt{\omega^2 - \mathbf{p}^2}) d\omega. \quad (\text{A.8})$$

## B Quasi-Carleman operators

We are interested in a class of Hankel operators, the so-called quasi-Carleman operators, defined as

$$(Af)(x) = \int_0^{\infty} A(x+x')f(x')dx' \quad (\text{B.1})$$

from the space of functions  $f \in L^2(\mathbb{R}^+)$  onto itself with kernels<sup>17</sup>

$$A(x+x') = \frac{1}{x+x'+r} e^{-\beta(x+x')}, \quad x, x' \geq 0. \quad (\text{B.2})$$

The spectrum and the eigenfunctions of these operators for  $r \geq 0$  and  $\beta = 0$ , and for  $r = 0$  and  $\beta > 0$  were derived many years ago [35–39], see also Ref. [40–42] for a review. Here we summarize the results relevant for the present paper only.

### B.1 The Carleman operator

The kernel of the Carleman operator is defined as in Eq. (B.2) with  $r = 0$  and  $\beta = 0$ . Since

$$A(t+t') = \frac{1}{t+t'} = \int_0^{\infty} e^{-\omega(t+t')} d\omega, \quad (\text{B.3})$$

by defining

$$u_s(t) = \frac{t^{is}}{\sqrt{2\pi t}}, \quad \lambda_s = \Gamma\left(\frac{1}{2} + is\right), \quad s \in \mathbb{R}, \quad (\text{B.4})$$

---

<sup>17</sup>We use the same symbol for operators and their kernels since the ambiguity is easily resolved from the context.

where  $\Gamma$  is the Euler gamma function [23], and by noticing that

$$\int_0^\infty u_s(\omega) e^{-\omega t} d\omega = \lambda_s u_s^*(t), \quad (\text{B.5})$$

it immediately follows that the  $u_s(t)$  diagonalize the Carleman operator

$$\int_0^\infty \frac{1}{t+t'} u_s(t') dt' = |\lambda_s|^2 u_s(t), \quad |\lambda_s|^2 = \frac{\pi}{\cosh(\pi s)}. \quad (\text{B.6})$$

The orthonormality of the basis functions can be proven by considering the change in the integration variable  $\eta = \log(t)$  so that

$$\int_0^\infty u_s^*(t) u_{s'}(t) dt = \int_{-\infty}^\infty e^{i\eta(s-s')} \frac{d\eta}{2\pi} = \delta(s-s'). \quad (\text{B.7})$$

The completeness is instead guaranteed by noticing that

$$\int_{-\infty}^\infty u_s^*(t) u_s(t') ds = \frac{\delta(\log(t/t'))}{\sqrt{tt'}} = \delta(t-t'), \quad (\text{B.8})$$

where  $\delta(t-t')$  on the r.h.s. indicates a representation of the  $\delta$ -function acting on the space of functions for which the Mellin transform and its inverse exist, see Appendix C.

In this basis, the kernel of the Carleman operator can be written in the diagonal form

$$A(t+t') = \int_{-\infty}^\infty |\lambda_s|^2 u_s(t) u_s^*(t') ds. \quad (\text{B.9})$$

Being the operator real, it is possible to choose a basis of real eigenfunctions

$$u_s^+(t) = \frac{u_s(t) + u_s^*(t)}{\sqrt{2}} = \frac{\cos(s \log(t))}{\sqrt{\pi t}}, \quad (\text{B.10})$$

$$u_s^-(t) = \frac{u_s(t) - u_s^*(t)}{\sqrt{2}i} = \frac{\sin(s \log(t))}{\sqrt{\pi t}}, \quad (\text{B.11})$$

with  $s \in \mathbb{R}^+$ . These functions satisfy the orthogonality relations

$$\int_0^\infty u_s^\pm(t) u_{s'}^\pm(t) dt = \delta(s-s'), \quad \int_0^\infty u_s^\pm(t) u_{s'}^\mp(t) dt = 0, \quad (\text{B.12})$$

while their completeness stems from

$$\int_0^\infty [u_s^+(t) u_s^+(t') + u_s^-(t) u_s^-(t')] ds = \delta(t-t'). \quad (\text{B.13})$$

In this basis, the kernel can be written as

$$A(t+t') = \int_0^\infty |\lambda_s|^2 [u_s^+(t) u_s^+(t') + u_s^-(t) u_s^-(t')] ds, \quad (\text{B.14})$$

making explicit the double degeneracy of the spectrum which originates from the fact that the kernel of  $A$  is singular when its argument approaches either zero or infinity, see for instance [43, 44]. Notice that, analogously to the case of the Fourier transform, the

two ensembles of  $u_s^+(t)$  and  $u_s^-(t)$  are bases for the even and odd functions under the transformation  $t \rightarrow 1/t$ , respectively. Indeed, to break the degeneracy of the spectrum, one can introduce the additional operator  $\mathcal{G}(t, t')$  by starting from Eq. (B.6) and by performing the change of variable  $t' \rightarrow 1/t'$  on the l.h.s so to obtain [43]

$$\int_0^\infty \mathcal{G}(t, t') u_s^\pm(t') dt' = \pm |\lambda_s|^2 u_s^\pm(t) \quad (\text{B.15})$$

with

$$\mathcal{G}(t, t') = \frac{1}{1+tt'} = \int_0^\infty |\lambda_s|^2 [u_s^+(t)u_s^+(t') - u_s^-(t)u_s^-(t')] ds. \quad (\text{B.16})$$

## B.2 The quasi-Carleman operator for $r = 0$ and $\beta > 0$

For  $r = 0$  and  $\beta = t_0 > 0$ , the kernel in Eq. (B.2) reads

$$A(\omega + \omega') = \frac{1}{\omega + \omega'} e^{-t_0(\omega + \omega')} = \int_{t_0}^\infty e^{-t(\omega + \omega')} dt. \quad (\text{B.17})$$

By defining

$$\hat{u}_s(\omega, t_0) = \frac{\sqrt{2s \sinh(\pi s)}}{\pi} \frac{K_{is}(\omega t_0)}{\sqrt{\omega}}, \quad t_0 > 0, \quad s \in \mathbb{R}^+, \quad (\text{B.18})$$

where  $K_\nu$  is the modified Bessel function of the second kind [23], from Eq. (6.627) of Ref. [23] it follows that

$$\int_0^\infty \frac{1}{\omega + \omega'} e^{-t_0(\omega + \omega')} \hat{u}_s(\omega', t_0) d\omega' = |\lambda_s|^2 \hat{u}_s(\omega, t_0), \quad \omega \geq 0, \quad t_0 > 0. \quad (\text{B.19})$$

The basis vectors  $\hat{u}_s(\omega, t_0)$  satisfy the orthonormality condition

$$\int_0^\infty \hat{u}_s(\omega, t_0) \hat{u}_{s'}(\omega, t_0) d\omega = \delta(s - s'), \quad (\text{B.20})$$

while their completeness stems from

$$\int_0^\infty \hat{u}_s(\omega, t_0) \hat{u}_s(\omega', t_0) ds = \delta(\omega - \omega') \quad \omega, \omega' \geq 0, \quad (\text{B.21})$$

where  $\delta(\omega - \omega')$  on the r.h.s. indicates a representation of the  $\delta$ -function acting on the space of functions for which the Kontorovich–Lebedev transform and its inverse exist, see Appendix C. The kernel of the quasi-Carleman operator in Eq. (B.17) can then be written in the diagonal form as

$$A(\omega + \omega') = \int_0^\infty |\lambda_s|^2 \hat{u}_s(\omega, t_0) \hat{u}_s(\omega', t_0) ds \quad (\text{B.22})$$

making explicit the non-degeneracy of the spectrum.

The Eq. (B.20) can be derived by starting from Eq. (6.576.4) of Ref. [23] which reads

$$\int_0^\infty \frac{K_{is}(\omega) K_{is'}(\omega)}{\omega^{1-\epsilon}} d\omega = \frac{2^{\epsilon-3}}{\Gamma(\epsilon)} \left| \Gamma\left(\frac{\epsilon + i(s + s')}{2}\right) \right|^2 \left| \Gamma\left(\frac{\epsilon + i(s - s')}{2}\right) \right|^2. \quad (\text{B.23})$$

By using  $\Gamma(z) = \Gamma(1+z)/z$ ,  $|\Gamma(is)|^2 = \pi/(s \sinh(\pi s))$ , and by noticing that the ratio  $\epsilon/[\pi((s-s')^2 + \epsilon^2)]$  is a representation of the  $\delta$ -function when  $\epsilon \rightarrow 0$ , one arrives at [45]

$$\lim_{\epsilon \rightarrow 0} \int_0^\infty \frac{K_{is}(\omega) K_{is'}(\omega)}{\omega^{1-\epsilon}} d\omega = \frac{\pi^2}{2s \sinh(\pi s)} \delta(s-s'), \quad (\text{B.24})$$

from which it follows Eq. (B.20). To understand how Eq. (B.21) can be derived, we start by defining

$$\begin{aligned} I_\epsilon(\omega, \omega') &= \int_0^\infty e^{-\epsilon s} \hat{u}_s(\omega, t_0) \hat{u}_s(\omega', t_0) ds \\ &= \frac{2}{\pi^2 \sqrt{\omega \omega'}} \int_0^\infty e^{-\epsilon s} s \sinh(\pi s) K_{is}(\omega t_0) K_{is}(\omega' t_0) ds \end{aligned} \quad (\text{B.25})$$

and, by using both representations in Eq. (9.6.22) of Ref. [26]

$$\begin{aligned} K_\nu(x) &= \frac{1}{\cos(\pi\nu/2)} \int_0^\infty \cos(x \sinh z) \cosh(\nu z) dz \\ &= \frac{1}{\sin(\pi\nu/2)} \int_0^\infty \sin(x \sinh z) \sinh(\nu z) dz, \end{aligned} \quad (\text{B.26})$$

it follows that

$$\begin{aligned} I_\epsilon(\omega, \omega') &= \frac{2}{\pi^2 \sqrt{\omega \omega'}} \int_0^\infty dz \int_0^\infty dz' \sin(\omega t_0 \sinh z) \cos(\omega' t_0 \sinh z') \times \\ &\quad \times \int_0^\infty e^{-\epsilon s} s \left[ \sin(s(z+z')) + \sin(s(z-z')) \right] ds. \end{aligned} \quad (\text{B.27})$$

By noticing that

$$\int_0^\infty e^{-\epsilon s} s \sin(\alpha s) ds = -\pi \frac{\partial}{\partial \alpha} \left( \frac{\epsilon/\pi}{\alpha^2 + \epsilon^2} \right), \quad (\text{B.28})$$

and by choosing  $\alpha = z \pm z'$ , by replacing the derivative with respect to  $\alpha$  with the one with respect to  $z$ , and by integrating by parts we then obtain

$$\begin{aligned} I_\epsilon(\omega, \omega') &= \frac{2t_0}{\pi} \sqrt{\frac{\omega}{\omega'}} \int_0^\infty dz \int_0^\infty dz' \cosh(z) \cos(\omega t_0 \sinh z) \cos(\omega' t_0 \sinh z') \times \\ &\quad \times \left[ \frac{\epsilon/\pi}{(z+z')^2 + \epsilon^2} + \frac{\epsilon/\pi}{(z-z')^2 + \epsilon^2} \right]. \end{aligned} \quad (\text{B.29})$$

We can now take the limit  $\epsilon \rightarrow 0$  to obtain

$$\lim_{\epsilon \rightarrow 0} I_\epsilon(\omega, \omega') = \frac{2t_0}{\pi} \sqrt{\frac{\omega}{\omega'}} \int_0^\infty \cos(\omega t_0 x) \cos(\omega' t_0 x) dx = \delta(\omega - \omega'), \quad (\text{B.30})$$

from which it follows Eq. (B.21).

### B.3 The quasi-Carleman operator for $r > 0$ and $\beta = 0$

For  $r = 2t_0 > 0$  and  $\beta = 0$ , the kernel in Eq. (B.2) reads

$$A(t+t') = \frac{1}{t+t'+2t_0} = \int_0^\infty e^{-\omega(t+t'+2t_0)} d\omega, \quad t, t' \geq 0. \quad (\text{B.31})$$

By defining

$$\begin{aligned} \bar{u}_s(t, t_0) &= \sqrt{\frac{s \tanh(\pi s)}{t_0}} P_{-\frac{1}{2}+is} \left( \frac{t}{t_0} \right) \\ &= \sqrt{\frac{s \tanh(\pi s)}{t_0}} {}_2F_1 \left( \frac{1}{2} + is, \frac{1}{2} - is; 1; \frac{t_0 - t}{2t_0} \right), \quad t \geq t_0 > 0 \quad s \in \mathbb{R}^+, \end{aligned} \quad (\text{B.32})$$

where  $P_\nu$  is the Legendre function and  ${}_2F_1$  is the Gauss's hypergeometric function [23], it follows that

$$\int_0^\infty \frac{1}{t+t'+2t_0} \bar{u}_s(t'+t_0, t_0) dt' = |\lambda_s|^2 \bar{u}_s(t+t_0, t_0), \quad t \geq 0, \quad (\text{B.33})$$

or equivalently

$$\int_{t_0}^\infty \frac{1}{t+t'} \bar{u}_s(t', t_0) dt' = |\lambda_s|^2 \bar{u}_s(t, t_0), \quad t \geq t_0. \quad (\text{B.34})$$

The basis vectors  $\bar{u}_s(t, t_0)$  satisfy the orthonormality condition

$$\int_{t_0}^\infty \bar{u}_s(t, t_0) \bar{u}_{s'}(t, t_0) dt = \delta(s - s'), \quad (\text{B.35})$$

while their completeness stems from

$$\int_0^\infty \bar{u}_s(t, t_0) \bar{u}_s(t', t_0) ds = \delta(t - t'), \quad t, t' \geq t_0 > 0, \quad (\text{B.36})$$

where  $\delta(t - t')$  on the r.h.s. indicates a representation of the  $\delta$ -function acting on the space of functions for which the Mehler-Fock transform and its inverse exist, see Appendix C. In this basis, the kernel of the quasi-Carleman operator in Eq. (B.31) can be written in the diagonal form as

$$A(t+t') = \int_0^\infty |\lambda_s|^2 \bar{u}_s(t, t_0) \bar{u}_s(t', t_0) ds, \quad t, t' \geq t_0 > 0 \quad (\text{B.37})$$

making explicit the non-degeneracy of the spectrum.

The Eqs. (B.34)-(B.36) can be derived directly from the analogous ones (B.19)-(B.21) in the previous subsection by noticing that, see Eqs. (6.621.3), (8.82) and (8.82.7) in Ref. [23] and Eq. (15.3.4) in Ref. [26], the  $\bar{u}_s(t, t_0)$  is the Laplace transform of  $\hat{u}_s(\omega, t_0)$ , i.e.

$$\int_0^\infty e^{-t\omega} \hat{u}_s(\omega, t_0) d\omega = |\lambda_s| \bar{u}_s(t, t_0). \quad (\text{B.38})$$

By computing an incomplete Laplace transform of the two sides of Eq. (B.38), and by using Eqs. (B.17) and Eq. (B.19), it follows that

$$\int_{t_0}^{\infty} e^{-\omega t} \bar{u}_s(t, t_0) dt = |\lambda_s| \hat{u}_s(\omega, t_0). \quad (\text{B.39})$$

The Eq. (B.34) can be derived<sup>18</sup> by performing the Laplace transform of both sides of Eq. (B.19), and then by using Eq. (B.17). The Eq. (B.35) is obtained by writing each of the  $\bar{u}_s(t, t_0)$  as in Eq. (B.38), and then by using Eqs. (B.17) and (B.19). A similar procedure applies to derive Eq. (B.36) from Eq. (B.21). For completeness we notice that Eqs. (B.35) and (B.36) can also be obtained with a derivation analogous to the one in Eqs. (B.23)–(B.30) [46].

## C Integral transforms

In this appendix we collect a few textbook formulas on the integral transforms that are used in the paper.

### C.1 Mellin transform

Given a function  $f(x)$  which is piecewise continuous for  $x \in \mathbb{R}^+$  and is of bounded variation in every finite subinterval, its Mellin transform<sup>19</sup> reads [21, 22]

$$\tilde{f}_s = \frac{1}{\sqrt{2\pi}} \int_0^{\infty} f(x) x^{s-1} dx = \int_0^{\infty} f(x) x^{q-1/2} u_s(x) dx, \quad (\text{C.1})$$

where  $\mathbf{s} \in \mathbb{C}$  is often defined as  $\mathbf{s} = q + is$  with  $q, s \in \mathbb{R}$ , while  $u_s(x)$  is given in Eq.(B.4). If

$$\lim_{x \rightarrow 0^+} f(x) = O(x^{-u}), \quad \lim_{x \rightarrow +\infty} f(x) = O(x^{-v}), \quad (\text{C.2})$$

then  $\tilde{f}_s$  exists in the “fundamental” open strip of the complex plane  $q \in (u, v)$ ,  $\tilde{f}_s$  depends analytically on  $\mathbf{s}$  in that strip, and then the inversion formula reads<sup>20</sup>

$$f(x) = \frac{1}{\sqrt{2\pi i}} \int_{q-i\infty}^{q+i\infty} \tilde{f}_s x^{-s} ds = x^{1/2-q} \int_{-\infty}^{+\infty} \tilde{f}_s u_s^*(x) ds, \quad q \in (u, v). \quad (\text{C.3})$$

One important property of the Mellin transform is the rescaling rule which states that the transform of  $g(x) = f(\mu x)$  is

$$\tilde{g}_s = \frac{1}{\mu^s} \tilde{f}_s, \quad \mu > 0. \quad (\text{C.4})$$

As an example relevant for this paper, the Mellin transform of the simple exponential

$$f(x) = \exp\{-x\} \quad \text{is} \quad \tilde{f}_s = \frac{\Gamma(\mathbf{s})}{\sqrt{2\pi}}, \quad (\text{C.5})$$

and is defined in the strip  $q \in (0, +\infty)$ .

<sup>18</sup>A direct derivation can also be obtained by using Eq. (B.32) and Eq. (7.512.10) in Ref. [23].

<sup>19</sup>With respect to the most common definition, we introduce a normalization factor  $1/\sqrt{2\pi}$ .

<sup>20</sup>For functions which are  $L^2(\mathbb{R}^+)$ , the  $u_s(x)$  are the basis functions of choice and  $q = 1/2$ .

## C.2 Kontorovich–Lebedev transform

The Kontorovich–Lebedev transform of a function  $f(\omega)$  is defined as<sup>21</sup> [41, 47–49]

$$\hat{f}_s = \int_0^\infty f(\omega) \hat{u}_s(\omega, t_0) d\omega, \quad s \in \mathbb{R}^+ \quad (\text{C.6})$$

where  $\hat{u}_s(\omega, t_0)$  is defined in Eq. (B.18). If  $f(\omega)$ , defined for  $\omega \in \mathbb{R}^+$ , is piecewise continuous, of bounded variation in every finite subinterval, and it satisfies

$$\lim_{\omega \rightarrow 0^+} f(\omega) = O(\omega^{-u}), \quad \lim_{\omega \rightarrow +\infty} f(\omega) = O(\omega^{-v}), \quad (\text{C.7})$$

then  $\hat{f}_s$  and the pointwise inversion formula exist if  $u < 1/2$  and  $v > 1$  [41]. By using the completeness relation of the basis functions (B.21), the inversion formula then reads

$$f(\omega) = \int_0^\infty \hat{f}_s \hat{u}_s(\omega, t_0) ds, \quad t_0 > 0. \quad (\text{C.8})$$

As a consequence, the functions which satisfy the conditions above are  $L^2(\mathbb{R}^+)$  but the viceversa is not true, i.e. not all the functions in  $L^2(\mathbb{R}^+)$  admit the inverse of the Kontorovich–Lebedev transform which requires a stronger convergence to zero at infinity.

## C.3 Mehler-Fock transform

The Mehler-Fock transform of a function  $f(t)$  [35, 41, 49, 50] is defined as<sup>22</sup>

$$\bar{f}_s = \int_{t_0}^\infty f(t) \bar{u}_s(t, t_0) dt, \quad s \in \mathbb{R}^+, \quad (\text{C.9})$$

where  $\bar{u}_s(t, t_0)$  is defined in Eq. (B.32). If  $f(t)$ , defined for  $t \geq t_0$ , is piecewise continuous, of bounded variation in every finite subinterval, and it satisfies

$$\lim_{t \rightarrow t_0^+} f(t) = O((t - t_0)^{-u}), \quad \lim_{t \rightarrow +\infty} f(t) = O(t^{-v}), \quad (\text{C.10})$$

then  $\bar{f}_s$  and the pointwise inversion formula exist if  $u < 1/4$  and  $v > 1/2$  [41]. By using the completeness relation of the basis functions (B.36), the inversion formula then reads

$$f(t) = \int_0^\infty \bar{f}_s \bar{u}_s(t, t_0) ds. \quad (\text{C.11})$$

As a consequence, the functions which satisfy the conditions above are  $L^2(t_0, \infty)$  but the viceversa is not true, i.e. not all the functions in  $L^2(t_0, \infty)$  admit the inverse of the Mehler-Fock transform which requires a weaker divergence in  $t_0$ .

---

<sup>21</sup>With respect to the standard definition which assumes  $t_0 = 1$ , we let the value of  $t_0 > 0$  be generic and leave the dependence on it implicit for the clarity of the presentation.

<sup>22</sup>We let again the value of  $t_0 > 0$  be generic and leave the dependence on it implicit.

## D Quasi-Carleman operators on discrete

With the intent of studying the discretized counterpart of the quasi-Carleman operators introduced in Appendix B, here we summarize known facts of the infinite Hilbert matrix [37–39] from which we derive properties of the discretized quasi-Carleman operators of interest for this paper.

### D.1 Hilbert matrix

The infinite Hilbert matrix

$$\mathcal{A}_{nn'} = \frac{1}{n + n' + \lambda}, \quad n, n' = 0, 1, 2, \dots, \quad \lambda \in \mathbb{R}, \quad \lambda \neq 0, -1, -2, \dots \quad (\text{D.1})$$

can be regarded as an operator acting on  $\ell^2(\mathbb{Z}^+)$ . We begin from its diagonalization [51]

$$\sum_{n'=0}^{\infty} A_{nn'} x_{n'}(\lambda, \mu) = \frac{\pi}{\sin(\pi\mu)} x_n(\lambda, \mu), \quad (\text{D.2})$$

where  $0 < \text{Re } \mu \leq 1/2$ , with the components of the eigenvectors given by

$$x_n(\lambda, \mu) = \sum_{k=0}^n \binom{n}{k} (-1)^k \frac{\Gamma(k + \mu)\Gamma(k + 1 - \mu)}{\Gamma(k + \lambda)\Gamma(k + 1)}, \quad n = 0, 1, 2, \dots \quad (\text{D.3})$$

By noticing that

$$\binom{n}{k} (-1)^k = \frac{(-n)_k}{k!} = \frac{1}{k!} (-n)(-n+1)\dots(-n+k-1), \quad (\text{D.4})$$

with the rising factorial (Pochhammer symbol) defined as

$$(x)_k = x(x+1)\dots(x+k-1), \quad (\text{D.5})$$

and by using the definition of the generalized hypergeometric series in Eq. (9.14.1) of Ref. [23], it is easy to show that

$$x_n(\lambda, \mu) = \frac{\Gamma(1 - \mu)\Gamma(\mu)}{\Gamma(\lambda)} {}_3F_2(-n, \mu, 1 - \mu; 1, \lambda; 1). \quad (\text{D.6})$$

For the case of interest,  $\mu = \frac{1}{2} + is$ , the eigenvalues in Eq. (D.2) coincide with those in the continuum, i.e.  $\pi/\sin(\pi\mu) = |\lambda_s|^2$ , see Eq. (B.6). To verify the completeness of the basis of eigenvectors, we notice that the  $x_n(\lambda, \frac{1}{2} + is)$  are related to the so-called continuous dual Hahn polynomials, defined as [52–54]

$$S_n(s^2; a, b, c) = (a + b)_n (a + c)_n {}_3F_2(-n, a + is, a - is; a + b, a + c, 1). \quad (\text{D.7})$$

They satisfy the orthogonality relation, see for instance Ref. [52],

$$\begin{aligned} \frac{1}{2\pi} \int_0^\infty ds |W_s(a, b, c)|^2 S_m(s^2; a, b, c) S_n(s^2; a, b, c) \\ = n! \Gamma(n + a + b) \Gamma(n + a + c) \Gamma(n + b + c) \delta_{nm}, \end{aligned} \quad (\text{D.8})$$

with

$$W_s(a, b, c) = \frac{\Gamma(a + is)\Gamma(b + is)\Gamma(c + is)}{\Gamma(2is)}. \quad (\text{D.9})$$

By choosing  $a = b = 1/2$  and  $c = \lambda - 1/2$ , we obtain the completeness relation for the normalized eigenvectors of the Hilbert matrix

$$\frac{1}{2\pi} \int_0^\infty \left| \frac{\Gamma(\lambda - 1/2 + is)}{\Gamma(2is)} \right|^2 x_n(\lambda, \frac{1}{2} + is) x_m(\lambda, \frac{1}{2} + is) ds = \delta_{nm}, \quad (\text{D.10})$$

from which one can verify explicitly the orthogonality condition

$$\sum_{n=0}^\infty x_n(\lambda, \frac{1}{2} + is) x_n(\lambda, \frac{1}{2} + is') = 2\pi \left| \frac{\Gamma(2is)}{\Gamma(\lambda - 1/2 + is)} \right|^2 \delta(s - s'). \quad (\text{D.11})$$

## D.2 Discretized quasi-Carleman operator for $r > 0$ and $\beta = 0$

We consider the discretization of the kernel of the quasi-Carleman operator in Eq. (B.31) defined as

$$\mathcal{A}(n + n') = \frac{1}{a(n + n') + 2t_0} = \int_0^\infty e^{-\omega(an + an' + 2t_0)} d\omega, \quad (n, n' = 0, 1, 2, \dots), \quad (\text{D.12})$$

where  $a$  is the lattice spacing. By using Eq. (D.2), we obtain

$$a \sum_{n'=0}^\infty \mathcal{A}(n + n') \bar{v}_s(n', t_0, a) = \sum_{n'=0}^\infty \frac{1}{n + n' + 2t_0/a} \bar{v}_s(n', t_0, a) = |\lambda_s|^2 \bar{v}_s(n, t_0, a), \quad (\text{D.13})$$

with  $s \in \mathbb{R}^+$  and, thanks to Eqs. (D.6), (D.11), and (D.12), the eigenvectors are given by

$$\bar{v}_s(n, t_0, a) = \sqrt{\frac{s \tanh(\pi s)}{t_0}} \frac{|\Gamma(2t_0/a - 1/2 + is)|}{\sqrt{a/(2t_0)} \Gamma(2t_0/a)} {}_3F_2\left(-n, \frac{1}{2} + is, \frac{1}{2} - is; 1, \frac{2t_0}{a}; 1\right). \quad (\text{D.14})$$

The Eq. (D.13) is the discretized version of Eq. (B.33) that we adopt. As expected, the eigenvalues of  $\mathcal{A}$  coincide with those in the continuum, i.e.  $|\lambda_s|^2$ , since for  $2t_0 = a$  the matrix  $\mathcal{A}(n + n')$  corresponds to a discrete representation of the quasi-Carleman operator in Eq. (B.17), see Ref. [27] for a recent review.

Thanks to Eqs. (D.10) and (D.11), the following completeness and orthogonality conditions hold

$$\int_0^\infty \bar{v}_s(n, t_0, a) \bar{v}_s(n', t_0, a) ds = a^{-1} \delta_{nn'}, \quad a \sum_{n=0}^\infty \bar{v}_s(n, t_0, a) \bar{v}_{s'}(n, t_0, a) = \delta(s - s'). \quad (\text{D.15})$$

*Continuum limit at fixed  $t_0$*

We study the approach to the continuum limit of  $\bar{v}_s(n, t_0, a)$  when  $t_0$  and  $t = an + t_0$  are kept constant. To this aim, we begin with the representation of the generalized hypergeometric series in Eq. (2.2.2) of Ref. [55]

$${}_3F_2\left(\lambda z, \frac{1}{2} + is, \frac{1}{2} - is; 1, \lambda; 1\right) = \frac{1}{|\lambda_s|^2} \int_0^1 x^{-\frac{1}{2} - is} (1-x)^{-\frac{1}{2} + is} {}_2F_1\left(\lambda z, \frac{1}{2} + is; \lambda; x\right) dx, \quad (\text{D.16})$$

where  $\lambda = 2t_0/a$  and  $z = (t - t_0)/(2t_0)$ . We then represent the Gauss hypergeometric function as in Eq. (3.197.1) of Ref. [23], but with the change of integration variable  $y \rightarrow y/(1-x)$ , i.e.

$${}_2F_1\left(\lambda z, \frac{1}{2} + is; \lambda; x\right) = \frac{\Gamma(\lambda)}{\lambda_s \Gamma(\lambda - \frac{1}{2} - is)} \int_0^\infty y^{-\frac{1}{2} + is} e^{-\lambda[z \log(1+(1-x)y) + (1-z) \log(1+y)]} dy. \quad (\text{D.17})$$

By noticing that the expression in the squared brackets at the exponent, for  $z < 0$  and  $x \in (0, 1)$ , has its minimum for  $y = 0$ , we use the Laplace method at the next-to-leading order in  $1/\lambda$  to obtain

$$\begin{aligned} {}_2F_1\left(\lambda z, \frac{1}{2} + is; \lambda; x\right) &= \frac{\Gamma(\lambda) \lambda^{-\frac{1}{2} - is}}{\Gamma(\lambda - \frac{1}{2} - is)} \times \\ &\times \left\{ \left[ 1 + \frac{1}{2\lambda} \left[ \frac{3}{4} + 2is - s^2 + z(1-z) \frac{\partial^2}{\partial z^2} \right] \right] (1-xz)^{-\frac{1}{2} - is} + O\left(\frac{1}{\lambda^2}\right) \right\}. \end{aligned} \quad (\text{D.18})$$

By inserting this equation in Eq. (D.16), using Eq. (9.111) in Ref. [23], and then plugging in the result in Eq. (D.14), we obtain

$$\bar{v}_s(n, t_0, a) = \frac{|\Gamma(\lambda - \frac{1}{2} + is)|}{\Gamma(\lambda - \frac{1}{2} - is)} \lambda^{-is} \left\{ \left[ 1 + \frac{1}{2\lambda} \left[ 1 + 2is + 2t \frac{\partial}{\partial t} \right] \right] \bar{u}_s(t, t_0) + O\left(\frac{1}{\lambda^2}\right) \right\}, \quad (\text{D.19})$$

where  $t = an + t_0$  and we have used the differential equation for the Legendre functions in Eq. (8.1.1) of Ref. [26]

$$\left[ (t_0^2 - t^2) \frac{\partial^2}{\partial t^2} - 2t \frac{\partial}{\partial t} - \frac{1}{4} - s^2 \right] \bar{u}_s(t, t_0) = 0. \quad (\text{D.20})$$

By using Eqs. (6.1.27) and (6.3.18) of Ref. [26] we obtain

$$\frac{|\Gamma(\lambda - \frac{1}{2} + is)|}{\Gamma(\lambda - \frac{1}{2} - is)} \lambda^{-is} = 1 - \frac{is}{\lambda} + O\left(\frac{1}{\lambda^2}\right), \quad (\text{D.21})$$

which finally leads to

$$\bar{v}_s(n, t_0, a) = \left\{ 1 + \frac{a}{4t_0} \left[ 1 + 2t \frac{\partial}{\partial t} \right] \right\} \bar{u}_s(t, t_0) + O(a^2), \quad (\text{D.22})$$

from which the derivative of  $\bar{v}_s(n, t_0, a)$  with respect to  $a$  in the limit  $a \rightarrow 0$  is readily obtained. As expected the basis vectors  $\bar{v}_s(n, t_0, a)$  tend to the continuum ones  $\bar{u}_s(t, t_0)$ , whereas discretization effects start at  $O(a)$ .

### D.3 Discretized quasi-Carleman operator for $r = 0$ and $\beta > 0$

By adopting a naive discretization of the integral on the r.h.s of Eq. (B.17), the kernel of that quasi-Carleman operator is modified as

$$\mathcal{A}(\omega + \omega') = \frac{a e^{-t_0(\omega + \omega')}}{1 - e^{-a(\omega + \omega')}} = a \sum_{n=0}^{\infty} e^{-(an+t_0)(\omega + \omega')}. \quad (\text{D.23})$$

The Eq. (B.19) is then replaced by

$$\int_0^\infty \frac{a e^{-t_0(\omega+\omega')}}{1 - e^{-a(\omega+\omega')}} \hat{v}_s(\omega', t_0, a) d\omega' = |\lambda_s|^2 \hat{v}_s(\omega, t_0, a), \quad \omega \geq 0, \quad t_0 > 0, \quad (\text{D.24})$$

with the eigenfunctions given by

$$\begin{aligned} \hat{v}_s(\omega, t_0, a) &= \frac{\sqrt{2s \sinh(\pi s)}}{\pi} \frac{|\Gamma(2t_0/a - 1/2 + is)|}{\sqrt{a/(2t_0)} \Gamma(2t_0/a)} \times \\ &\times \sqrt{\frac{\pi}{2t_0}} e^{-\omega t_0} \frac{a}{1 - e^{-a\omega}} {}_2F_1\left(\frac{1}{2} + is, \frac{1}{2} - is; \frac{2t_0}{a}; -\frac{e^{-a\omega}}{1 - e^{-a\omega}}\right). \end{aligned} \quad (\text{D.25})$$

The  $\hat{v}_s(\omega, t_0, a)$  and  $\bar{v}_s(t, t_0, a)$  are related by the equation

$$a \sum_{n=0}^{\infty} e^{-\omega(an+t_0)} \bar{v}_s(n, t_0, a) = |\lambda_s| \hat{v}_s(\omega, t_0, a) \quad (\text{D.26})$$

which is a discretized version of the Laplace transform in Eq. (B.39). It can be derived by combining Eqs. (D.3) and (D.6) so to have

$$\begin{aligned} \sum_{n=0}^{\infty} \zeta^n {}_3F_2(-n, \mu, 1-\mu; 1, \lambda; 1) &= \frac{\Gamma(\lambda)}{\Gamma(1-\mu)\Gamma(\mu)} \sum_{k=0}^{\infty} (-1)^k \frac{\Gamma(k+\mu)\Gamma(k+1-\mu)}{\Gamma(k+\lambda)\Gamma(k+1)} \sum_{n=k}^{\infty} \binom{n}{k} \zeta^n \\ &= \frac{1}{1-\zeta} {}_2F_1\left(\mu, 1-\mu; \lambda; -\frac{\zeta}{1-\zeta}\right), \end{aligned} \quad (\text{D.27})$$

where we have used the identity

$$\sum_{n=k}^{\infty} \binom{n}{k} \zeta^n = \frac{\zeta^k}{(1-\zeta)^{k+1}} \quad (\text{D.28})$$

obtained by deriving  $k$  times the summation of the geometric series with respect to  $\zeta$ . Then Eq. (D.25) is obtained from Eqs. (15.1.1) in Ref. [26] by choosing  $\zeta = e^{-a\omega}$ .

The Eq. (D.24) can easily be derived by starting from Eq. (D.13), by representing the kernel as on the r.h.s of Eq. (D.12), then by performing a discrete Laplace transform on both sides of the equation, and finally by using Eq. (D.23). By performing the Laplace transform on both sides of Eq. (D.26), and by using Eqs. (D.12) and Eq. (D.13) it follows that

$$\int_0^\infty e^{-(an+t_0)\omega} \hat{v}_s(\omega, t_0, a) d\omega = |\lambda_s| \bar{v}_s(n, t_0, a), \quad (\text{D.29})$$

the analogous of Eq. (B.38). By using Eqs. (D.12) and (D.13), and the completeness and orthonormality conditions in Eq. (D.15) it follows that

$$\int_0^\infty \hat{v}_s(\omega, t_0, a) \hat{v}_{s'}(\omega, t_0, a) d\omega = \delta(s-s'), \quad \int_0^\infty \hat{v}_s(\omega, t_0, a) \hat{v}_s(\omega', t_0, a) ds = \delta(\omega-\omega'), \quad (\text{D.30})$$

where  $\delta(\omega-\omega')$  on the r.h.s. indicates a representation of the  $\delta$ -function acting on the space of functions for which Eq. (5.1) can be uniquely inverted.

*Continuum limit at fixed  $t_0$*

To study the approach to the continuum limit of the functions  $\hat{v}_s(\omega, t_0, a)$  defined in Eq. (D.25), we start from Eq. (15.4.16) of Ref. [26] which, by defining  $\lambda = 2t_0/a$ , reads

$${}_2F_1\left(\frac{1}{2} + is, \frac{1}{2} - is; \lambda; -\frac{e^{-2\omega t_0/\lambda}}{1 - e^{-2\omega t_0/\lambda}}\right) = \Gamma(\lambda) e^{\omega t_0} e^{-\omega t_0/\lambda} P_{-\frac{1}{2}-is}^{1-\lambda}\left(\coth\left(\frac{\omega t_0}{\lambda}\right)\right). \quad (\text{D.31})$$

Thanks to Eq. (8.713.3) of Ref. [23], the associated Legendre function of first kind can be represented as

$$P_{-\frac{1}{2}-is}^{1-\lambda}(z) = \sqrt{\frac{2}{\pi}} \frac{\Gamma(\bar{\lambda})}{|\Gamma(\bar{\lambda} - is)|^2} J(z, \bar{\lambda}), \quad \bar{\lambda} = \lambda - \frac{1}{2}, \quad z = \coth\left(\frac{\omega t_0}{\lambda}\right), \quad (\text{D.32})$$

where

$$J(z, \bar{\lambda}) = (z^2 - 1)^{\frac{\bar{\lambda}}{2} - \frac{1}{4}} \int_0^\infty \cosh(isx) e^{-\bar{\lambda} \log(z + \cosh x)} dx. \quad (\text{D.33})$$

By defining  $y^2 = (\cosh x - 1)$ , then

$$J(z, \bar{\lambda}) = 2(z^2 - 1)^{\frac{\bar{\lambda}}{2} - \frac{1}{4}} \int_0^\infty \cosh(isx(y)) e^{-\bar{\lambda} \log(z+1+y^2)} \frac{dy}{\sqrt{2+y^2}}, \quad (\text{D.34})$$

and by using the Laplace method at the next-to-leading order in  $1/\bar{\lambda}$  we obtain

$$J(z, \bar{\lambda}) = (z^2 - 1)^{\frac{\bar{\lambda}}{2} - \frac{1}{4}} (z + 1)^{-\bar{\lambda}} e^\alpha \times \left\{ \left[ 1 + \frac{\bar{\lambda}}{2(z+1)^2} \left[ 1 + 2\frac{\partial}{\partial \alpha} + \frac{\partial^2}{\partial \alpha^2} \right] \right] K_{is}(\alpha) \Big|_{\alpha=\frac{\bar{\lambda}}{z+1}} + O\left(\frac{1}{\bar{\lambda}^2}\right) \right\}, \quad (\text{D.35})$$

where we have used the integral representation of the modified Bessel function in Eq. (9.6.24) of Ref. [26]

$$K_{is}(\alpha) = \int_0^\infty \cosh(isx) e^{-\alpha \cosh x} dx. \quad (\text{D.36})$$

By expanding the various terms in  $1/\lambda$ , we obtain

$$J(z, \bar{\lambda}) = \sqrt{\frac{t_0}{\lambda}} \left\{ \omega \left[ 1 - \frac{1}{2\lambda} \left[ 1 + s^2 + 2\omega \frac{\partial}{\partial \omega} \right] \right] \frac{K_{is}(\omega t_0)}{\sqrt{\omega}} + O\left(\frac{1}{\lambda^2}\right) \right\}, \quad (\text{D.37})$$

where we have used the differential equation for the modified Bessel function in Eq. (9.6.1) of Ref. [26]

$$\left[ \omega^2 \frac{\partial^2}{\partial \omega^2} + \omega \frac{\partial}{\partial \omega} - (\omega t_0)^2 + s^2 \right] K_{is}(\omega t_0) = 0. \quad (\text{D.38})$$

By expanding at the next-to-leading order in  $1/\lambda$  the prefactors in Eqs. (D.25) and (D.32), and by setting  $\lambda = 2t_0/a$  we finally obtain

$$\hat{v}_s(\omega, t_0, a) = \left\{ 1 - \frac{a}{4t_0} \left[ 1 + 2\omega \frac{\partial}{\partial \omega} \right] \right\} \hat{u}_s(\omega, t_0) + O(a^2), \quad (\text{D.39})$$

from which the derivative of  $\hat{v}_s(\omega, t_0, a)$  with respect to  $a$  in the limit  $a \rightarrow 0$  is readily obtained. As expected the basis vectors  $\hat{v}_s(\omega, t_0, a)$  tend to the continuum ones  $\hat{u}_s(\omega, t_0)$ , whereas discretization effects start at  $O(a)$ . As further checks, we have verified that, order by order, the r.h.s. of Eq. (D.22) is obtained from the r.h.s. of Eq. (D.39) by using Eq. (D.29) and viceversa by using Eq. (D.26).

## E Alternative strategy for (smeared) regulated spectral densities

In this appendix, we present an alternative method to compute the regulated spectral density  $\rho_m(\omega)$ . The idea is to modify the ultraviolet behavior of  $C(t)$  so that, in the presence of a mass gap, the modified correlation function

$$C_{(m)}(t) = C(t) t^m = \int_0^\infty \rho(\omega) \left(-\frac{\partial}{\partial \omega}\right)^m e^{-\omega t} d\omega = \int_0^\infty \rho_{(m)}(\omega) e^{-\omega t} d\omega \quad (\text{E.1})$$

is associated to the spectral density

$$\rho_{(m)}(\omega) = \frac{\partial^m}{\partial \omega^m} [\rho(\omega)] = \frac{\partial^m}{\partial \omega^m} [\omega^m \rho_m(\omega)]. \quad (\text{E.2})$$

This relation can be inverted similarly to Eq. (2.31). By noticing that, in the presence of a mass gap,  $\rho_m(\omega)$  and its derivatives vanish at  $\omega = 0$ , then the regulated spectral density can be obtained as

$$\rho_m(\omega) = \frac{1}{\Gamma(m) \omega^m} \int_0^\omega \rho_{(m)}(\omega') (\omega - \omega')^{m-1} d\omega'. \quad (\text{E.3})$$

The smeared spectral density  $\rho_{\kappa;m}$ , see Eq. (3.1), directly follows from integrating  $\rho_m(\omega)$ , written as in Eq. (E.3), with  $\kappa(\omega)$

$$\rho_{\kappa;m} = \int_0^\infty \rho_{(m)}(\omega) \kappa_{(m)}(\omega) d\omega, \quad (\text{E.4})$$

where

$$\kappa_{(m)}(\omega) = \frac{1}{\Gamma(m)} \int_\omega^\infty \kappa(\omega') \frac{(\omega' - \omega)^{m-1}}{\omega'^m} d\omega'. \quad (\text{E.5})$$

For the Breit-Wigner kernel considered in this work, see Eq. (3.4), this integral amounts to

$$\kappa_{(m)}(\omega) = \frac{1}{\pi \Gamma(1+m) \omega} \text{Im} \left\{ {}_2F_1 \left( 1, 1; 1+m; \frac{\omega_* + i\sigma}{\omega} \right) \right\}, \quad (\text{E.6})$$

where in the derivation Eqs. (3.197.2) and (15.3.3) of Refs. [23] and [26] have been used, respectively.

## References

- [1] E.C. Poggio, H.R. Quinn and S. Weinberg, *Smearing the Quark Model*, *Phys. Rev. D* **13** (1976) 1958.
- [2] S. Weinberg, *The Quantum theory of fields. Vol. 1: Foundations*, Cambridge University Press (6, 2005), [10.1017/CBO9781139644167](https://doi.org/10.1017/CBO9781139644167).
- [3] M.T. Hansen, H.B. Meyer and D. Robaina, *From deep inelastic scattering to heavy-flavor semileptonic decays: Total rates into multihadron final states from lattice QCD*, *Physical Review D* **96** (2017) .
- [4] P. Gambino and S. Hashimoto, *Inclusive Semileptonic Decays from Lattice QCD*, *Phys. Rev. Lett.* **125** (2020) 032001 [[2005.13730](https://arxiv.org/abs/2005.13730)].

- [5] S. Jeon and L.G. Yaffe, *From quantum field theory to hydrodynamics: Transport coefficients and effective kinetic theory*, *Phys. Rev. D* **53** (1996) 5799 [[hep-ph/9512263](#)].
- [6] H.B. Meyer, *A Calculation of the shear viscosity in  $SU(3)$  gluodynamics*, *Phys. Rev. D* **76** (2007) 101701 [[0704.1801](#)].
- [7] FLAVOUR LATTICE AVERAGING GROUP (FLAG) collaboration, *FLAG review 2024*, *Phys. Rev. D* **113** (2026) 014508 [[2411.04268](#)].
- [8] R. Aliberti et al., *The anomalous magnetic moment of the muon in the Standard Model: an update*, *Phys. Rept.* **1143** (2025) 1 [[2505.21476](#)].
- [9] M. Cè, L. Giusti and S. Schaefer, *Domain decomposition, multi-level integration and exponential noise reduction in lattice QCD*, *Phys. Rev. D* **93** (2016) 094507 [[1601.04587](#)].
- [10] M. Cè, L. Giusti and S. Schaefer, *A local factorization of the fermion determinant in lattice QCD*, *Phys. Rev. D* **95** (2017) 034503 [[1609.02419](#)].
- [11] M. Dalla Brida, L. Giusti, T. Harris and M. Pepe, *Multi-level Monte Carlo computation of the hadronic vacuum polarization contribution to  $(g_\mu - 2)$* , *Phys. Lett. B* **816** (2021) 136191 [[2007.02973](#)].
- [12] M. Lüscher, *Stochastic locality and master-field simulations of very large lattices*, *EPJ Web Conf.* **175** (2018) 01002 [[1707.09758](#)].
- [13] L. Giusti and M. Lüscher, *Topological susceptibility at  $T > T_c$  from master-field simulations of the  $SU(3)$  gauge theory*, *Eur. Phys. J. C* **79** (2019) 207 [[1812.02062](#)].
- [14] A. Francis, P. Fritzscht, M. Lüscher and A. Rago, *Master-field simulations of  $O(a)$ -improved lattice QCD: Algorithms, stability and exactness*, *Comput. Phys. Commun.* **255** (2020) 107355 [[1911.04533](#)].
- [15] M. Hansen, A. Lupo and N. Tantalo, *Extraction of spectral densities from lattice correlators*, *Physical Review D* **99** (2019) .
- [16] G. Bailas, S. Hashimoto and T. Ishikawa, *Reconstruction of smeared spectral function from Euclidean correlation functions*, *PTEP* **2020** (2020) 043B07 [[2001.11779](#)].
- [17] M. Bruno, L. Giusti and M. Saccardi, *Spectral densities from Euclidean lattice correlators via the Mellin transform*, *Phys. Rev. D* **111** (2025) 094515 [[2407.04141](#)].
- [18] L. Giusti et al., *in preparation*.
- [19] J. Bulava and M.T. Hansen, *Scattering amplitudes from finite-volume spectral functions*, *Phys. Rev. D* **100** (2019) 034521 [[1903.11735](#)].
- [20] A. Patella and N. Tantalo, *Scattering amplitudes from Euclidean correlators: Haag-Ruelle theory and approximation formulae*, *JHEP* **01** (2025) 091 [[2407.02069](#)].
- [21] R. Wong, *Asymptotic Approximations of Integrals*, SIAM - Academic Press, New York (8, 2001), [10.1137/1.9780898719260](#).
- [22] P. Flajolet, X. Gourdon and P. Dumas, *Mellin transforms and asymptotics: Harmonic sums*, *Theoretical Computer Science* **144** (1995) 3.
- [23] I.S. Gradshteyn, I.M. Ryzhik, D. Zwillinger and V. Moll, *Table of integrals, series, and products; 8th ed.*, Academic Press, Amsterdam (2015), [0123849330](#).
- [24] EXTENDED TWISTED MASS collaboration, *Inclusive hadronic decay rate of the  $\tau$  lepton from lattice QCD*, *Phys. Rev. D* **108** (2023) 074513 [[2308.03125](#)].

- [25] EXTENDED TWISTED MASS collaboration, *Inclusive hadronic decay rate of the  $\tau$  lepton from lattice QCD: The  $\bar{u}s$  flavor channel and the cabibbo angle*, *Phys. Rev. Lett.* **132** (2024) 261901 [[2403.05404](#)].
- [26] M. Abramowitz and I.A. Stegun, *Handbook of Mathematical Functions*, Dover Publications Inc., New York (1965).
- [27] D.R. Yafaev, *Hankel and Toeplitz operators: continuous and discrete representations*, *Opuscula Math.* **37** (2017) 189 [[1607.04988](#)].
- [28] R. Tsuji and S. Hashimoto, *Spectral reconstruction from Euclidean lattice correlators through singular value decomposition*, [2605.15674](#).
- [29] S. Lawrence, *Model-free spectral reconstruction via Lagrange duality*, [2408.11766](#).
- [30] R. Abbott, S. Fields, W.I. Jay, P. Oare and M. Saccardi, *The Causal Bootstrap: Bounding Smeared Spectral Functions from Non-Perturbative Euclidean Data*, [2605.20509](#).
- [31] W.I. Jay and M. Saccardi, *Kernel transformations and bounds for smeared spectral functions*, [2606.19503](#).
- [32] F.A. Bresciani, M. Bruno and M.T. Hansen, *Finite-volume effects on smeared spectral densities*, [2606.14349](#).
- [33] R. Kellermann, Z. Hu, A. Barone, A. Elgaziari, S. Hashimoto, T. Kaneko et al., *Inclusive semileptonic decays from lattice QCD: Analysis of systematic effects*, *Phys. Rev. D* **112** (2025) 014501 [[2504.03358](#)].
- [34] G. Morandi, M. Bruno, F.A. Bresciani, C. Lehner and J. Parrino, *Towards the time-like pion form factor beyond the elastic regime using domain-wall QCD*, in *42th International Symposium on Lattice Field Theory*, 3, 2026 [[2603.04094](#)].
- [35] F.G. Mehler, *Ueber eine mit den Kugel- und Cylinderfunctionen verwandte Function und ihre Anwendung in der Theorie der Elektrizitätsvertheilung*, *Math. Ann.* **18** (1881) 161.
- [36] T. Carleman, *Sur les équations intégrales singulières à noyau réel et symétrique*, Uppsala universitets årsskrift, Matematik och naturvetenskap (1923).
- [37] W. Magnus, *On the spectrum of Hilbert's Matrix*, *American Journal of Mathematics* **72**, No. 4 (1950) 699.
- [38] M. Rosenblum, *On the Hilbert matrix, I*, *Proceedings of the American Mathematical Society* **9** (1958) 137.
- [39] M. Rosenblum, *On the Hilbert matrix, II*, *Proceedings of the American Mathematical Society* **9** (1958) 581.
- [40] E. Titchmarsh, *Eigenfunction Expansions Associated With Second Order Differential Equations*, Oxford At The Clarendon Press (1946).
- [41] N.N. Lebedev, *Special Functions and Their Applications, revised edn*, Dover Publications, Inc., New York (1972) (1965).
- [42] D.R. Yafaev, *Quasi-Carleman Operators and Their Spectral Properties*, *Integr. Equ. Oper. Theory* **81** (2015) 499 [[1404.6742](#)].
- [43] J.S. Howland, *Spectral theory of operators of Hankel type, II*, *Indiana University Mathematics Journal* **41** (1992) 427.

- [44] D.R. Yafaev, *A Commutator Method for the Diagonalization of Hankel Operators*, *Functional Analysis and Its Applications* **44** (2010) 295.
- [45] A. A. Passian, H. Simpson, S. Kouckekian and S. Yakubovich, *On the orthogonality of the MacDonal'd's functions*, *J. Math. Anal. Appl.* **360** (2009) 380.
- [46] I.H. Sneddon, *The use of Integral transforms*, McGraw-Hill, New York (1972).
- [47] L.N. Kontorovich M. I., *On the one method of solution for some problems in diffraction theory and related problems*, *J. Exp. Theor. Phys.* **8(10-11)** (1938) 1192.
- [48] L.N. Kontorovich M. I., *On the application of inversion formulae to the solution of some electrodynamic problems*, *J. Exp. Theor. Phys.* **9(6)** (1939) 729.
- [49] H.J. Glaeske, A. Prudnikov and K.A. Skórník, *Operational Calculus and Related Topics*, Analytical Methods and Special Functions Series, Chapman & Hall/CRC (2006).
- [50] V.A. Fock, *On the representation of an arbitrary function by an integral involving Legendre's functions with a complex index*, *Acad. Sci. URSS* (1943) 253–256.
- [51] C.K. Hill, *On the Singly-Infinite Hilbert Matrix*, *Journal of the London Mathematical Society* **s1-35** (1960) 17.
- [52] R. Koekoek, P. Lesky and R. Swarttouw, *Hypergeometric Orthogonal Polynomials and Their  $q$ -Analogues*, Springer Monographs in Mathematics, Springer Berlin Heidelberg (01, 2010), [10.1007/978-3-642-05014-5](https://doi.org/10.1007/978-3-642-05014-5).
- [53] E. Neuman, *On Hahn polynomials and continuous dual Hahn polynomials*, *Journal of Computational Analysis and Applications* **8** (2006) 229.
- [54] T.H. Koornwinder, *Group theoretic interpretations of Askey's scheme of hypergeometric orthogonal polynomials*, in *Orthogonal Polynomials and their Applications*, M. Alfaro, J.S. Dehesa, F.J. Marcellan, J.L. Rubio de Francia and J. Vinuesa, eds., (Berlin, Heidelberg), pp. 46–72, Springer Berlin Heidelberg, 1988.
- [55] G.E. Andrews, R. Askey and R. Roy, *Special Functions*, Cambridge University Press (1999).